Creation of phantom sources using adaptive filters

van der Tol, F.J.C.

Award date:
1995

Creation of phantom sources using adaptive filters

F.J.C. van der Tol

Eindhoven, August 1995

Eindhoven University of Technology
Faculty of Electrical Engineering
Electronic Circuit Design Group (EEB)

Head of department	prof. dr. ir. W.M.G. van Bokhoven
EUT-supervisor	dr. ir. P.C.W. Sommen
NatLab-group leader	dr. ir. P.J. Otterloo
NatLab-supervisor	ing. R.M. Aarts

"Homo sum, humani nil a me alienum puto"
I am human and am therefore indifferent to nothing done by humans.
Ik ben mens en acht niets menselijk mij vreemd.
Terentius.

Acknowledgements

The work described in this report was conducted at the DSP group of Philips Research Laboratories in Eindhoven. I would especially like to thank the following people for their contribution:
My university supervisor Piet Sommen for bringing me in contact with Philips and guiding me thoughout the project, Ronald Aarts for the coaching and for the many suggestions he made during this project. Paul Boers for his patience during his explanations of the hardware and Simon Webster for helping with experiments and correcting this report.

Summary

A listener positioned up in front of two loudspeakers can sense the direction from which the sound is coming due to the directional information it contains. It is however possible to alter the sound coming from the speakers so that it appears to come from another direction. If this is the case one speaks of "phantom sources". If phantom sources are created using fixed filters to alter the sound, this phenomenon only works for one position in space (the environment). If the situation changes, for example the position of the listener, another filter must be used. This problem can be solved when, instead of a fixed filter, an *adaptive filter* is used. This filter tries to compensate the difference due to the changing of the position so the optimal perception is again achieved.

The idea applied for creating phantom sources using adaptive filter(s) is based on what is known as Active Noise Control. Here secondary sound sources are driven by adaptive controllers which aims to introduce a cancelling signal so that a primary field is compensated in certain places in an enclosure. Active noise control utilizes the filtered-x algorithm, which is an alternated form of the well known LMS algorithm in situations where a transfer function in the auxiliary path following the adaptive filter. To ensure convergence of this algorithm, the input to the update mechanism has to be filtered by a copy of the plant transfer function. In the case of active noise control the auxiliary path of the adaptive filter consists of the transfer function between secondary source(s) and microphone(s).

The first part of this report gives a brief overview of how phantom sources are created using fixed filters and in what manner it can be done using an adaptive system. Then after an introduction to adaptive filters and their properties, a model is derived describing the filtered-x algorithm and it is shown that, under certain conditions this algorithm is stable and converges to the optimal solution. After this, results from real time experiments, utilizing the filtered-x algorithm in a single point cancellation setup are presented to show the power reduction obtained when one secondary source is used to cancel out the disturbance produced by a primary source.

In order to simulate an observer, two sensors are needed representing the left and right ear. Therefore a multiple error LMS algorithm is presented which minimizes the sum of the mean squared of a number of error sensors. The algorithm is, again, tested in a real time environment, where this time two secondary sources are used to cancel a single primary source in the vicinity of two microphones. After this a more realistic setup is used, where

the two microphones are replaced by a B & K dummy head representing the observer.
Next, the secondary speakers which were, until now, placed in front of the "subject" are replaced by headphones in order to see if the problem of In the Head-Locatedness could be solved using this system. Results from experiments conducted, using a headphone with small built-in microphones are shown.

Contents

Chapter 1

Introduction

When a listener is placed in front of two loudspeakers, serving as sound sources, he/she will perceive sound due to the physical nature of propagation of acoustic waves. This sound contains directional information, so the listener is capable of sensing the direction from which the sound signals originate. It is possible however, to alter the sound coming from the speakers so that it appears to come from another direction. In such a case one speaks of "*phantom sound sources*". A phantom sound source is a sources which is precieved by the listener to come from a point other than that of the actual sound source.
The creation of phantom sound sources or sound broadening systems using a fixed set of filters is already a well studied topic and nowadays several companies have commercialised their designs. Recently, Philips Research and Development designed a system called "Incredible Sound" which broadens the stereo sound field when a set of speakers is placed close together. This design has already proven useful for sound improvement in televisions where the speakers are normally placed close together.
If phantom sound sources are created using fixed filters, the phenomena only works for one position in space (the environment). If the situation changes, for example the position of the listener, another filter should be used. This problem can be solved when instead of a fixed filter, an adaptive filter is used. This filter tries to compensate the difference due to changes of the position so that the optimal perception is reached again.
The changing position of the listener is not the only problem which occurs when using fixed filters for the creation of phantom sound sources. The determination of the filters itself causes some practical and mathematical difficulties. Before a set of filters can be ascertained, up to eight transfer functions have to be measured to create two virtual sound sources. After these measurements some mathematical operation have to be applied which include multiplying, dividing, rounding and stabilizing the resultant transfer functions. This makes the creation of phantom sound sources using a fixed set of filters very time consuming especially when several different angles of perception have to be realized.
Another application in which a sound broadening system can be used is a

situation where the sound field is produced by a headphone. When a subject listens to music via earphones, the sound always appears to be coming from within the head. This phenomena is already a well studied topic and is known as In-the-Head Locatedness or short IHL. By processing the signals applied to the headphone speakers it might be possible to overcome this problem and produce sound so that the subject perceives an out-of-the head auditory event.
Engineering problem will be assessed when phantom sources are created using adaptive filters. The first part will give a closer look at the method used until now and the practical problems that arise when using this technique. Then a theoretical analysis is given on the creation of an adaptive system to create phantom sound sources and the limitations it has. Results from practical experiments will be presented to illustrate the behavior of the adaptive system.In this report the engineering problem will be assessed when phantom sources are created using adaptive filters. The first part will give a closer look at the method used until now and the practical problems that arise when using this technique. Then a theoretical analysis is given on the creation of an adaptive system to create phantom sound sources and the limitations it has. Results from practical experiments will be presented to illustrate the behavior of the adaptive system.

1.1 Generation of phantom sources using fixed filters

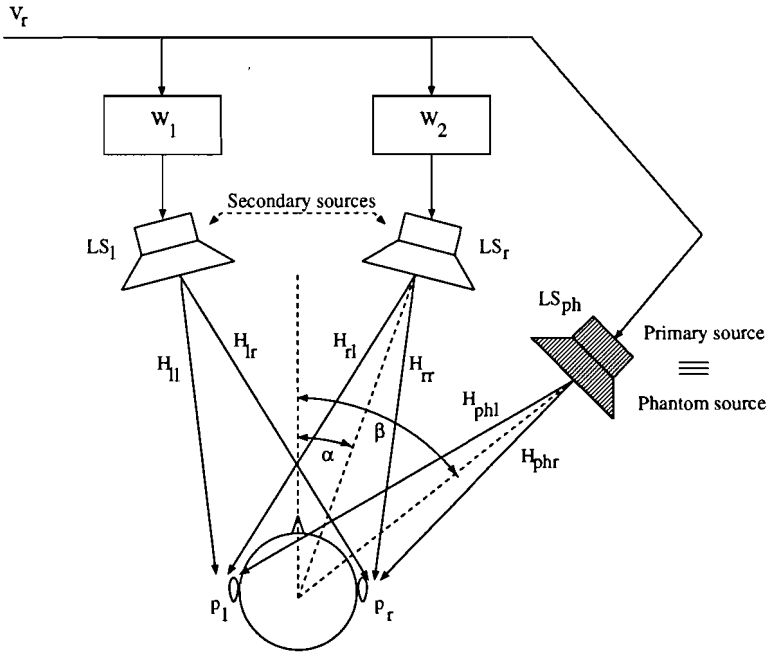

Figure 1.1: Creation of phantom sources using fixed filters.

Fig. 1.1 shows a situation where an observer is placed in front of two loudspeakers, LS_l and LS_r, serving as secondary source at an angle α. In order to create a phantom sound source, LS_{ph} at angle β, the input signal V_r is processed so the pressure in the ears of the observer created by the secondary sources is equal to the pressure in the ears produced by the primary or phantom source. Mathematically, this problem is very easy to solve. The pressure in the ears caused by the secondary sources is given by:

$$p_l = V_r \left(W_1 H_{ll} + W_2 H_{rl}\right) \tag{1.1}$$

and

$$p_r = V_r \left(W_1 H_{lr} + W_2 H_{rr}\right), \tag{1.2}$$

where W_1 and W_2 are the (unknown) fixed filters. The transfer function H_{lr} is from left loudspeaker to the right ear. The other functions used are as illustrated in Fig. 1.1 with the first index corresponding to the source and the second index to the ear. The pressure at the ears caused by the phantom source LS_{ph} is

$$p_l = V_r H_{phl} \tag{1.3}$$

and

$$p_r = V_r H_{phr}. \tag{1.4}$$

Combining Eqs. (1.1),(1.2),(1.3) and (1.4) and solving the set of simultaneous equations results in:

$$\begin{aligned} W_1 &= \frac{H_{phl}H_{rr} - H_{phr}H_{rl}}{H_{ll}H_{rr} - H_{lr}H_{rl}}, \\ W_2 &= \frac{H_{phl}H_{lr} - H_{phr}H_{ll}}{H_{lr}H_{rl} - H_{ll}H_{rr}}. \end{aligned} \tag{1.5}$$

When the transfer functions calculated with Eq.1.5 are placed in front of the secondary sources LS_l and LS_r, the pressure at the ears of the subject is the same as would be obtained when only the phantom source on the right of the subject was playing. Hence using these filters will accomplish a virtual enlargement of the aperture from α to β. The same can be done for a virtual source at the left side of the subject resulting in a stereophonic broadening system.
Theoretically this all seems very clear. Practically however, there are some problems to be solved. Since pressure is not a direct measurable quantity, microphones have to be used to transform this into an electric signal.

The transfer functions H_{ll}, H_{lr}, H_{rl} and H_{rr} are measured using a test subject in e.g. an anechoic room. Due to possible changes in the position of the head during these measurements, errors are introduced. Then mathematical manipulations such as multiplying, adding and dividing have to be performed on these functions to yield the desired filters W_1 and W_2. Again some errors are introduced since the resulting function is most likely not stable. Next a suitable model for the fixed filters has to be chosen and

the mathematical solution has to be fitted within this model again introducing errors. The obtained solution will vary depending on used model, used method to stabilize functions and head movement during measurement. To find the best possible solution, that is the solution for which the test subject perceives the sound from the phantom source position several different models should be tested.

1.2 Generation of phantom sources using adaptive filters

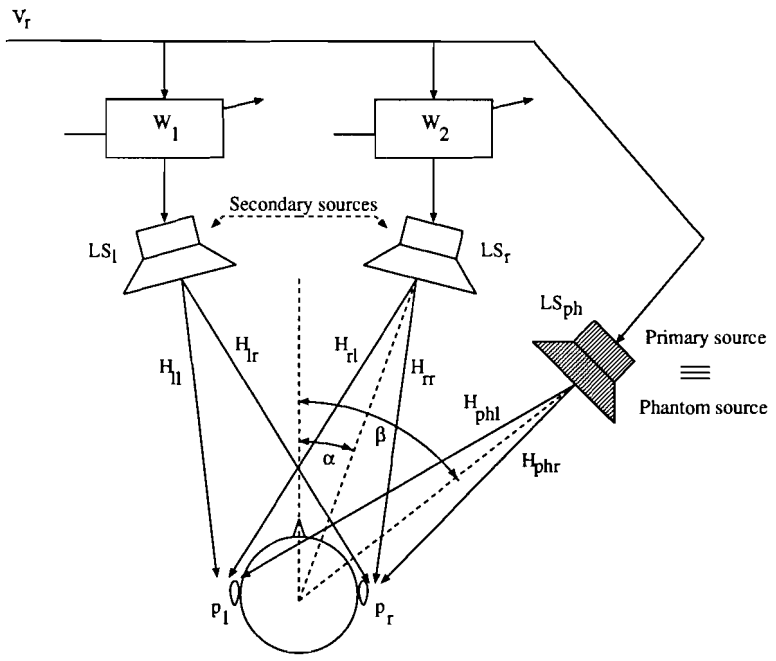

Figure 1.2: Creation of phantom sources using adaptive filters.

The idea of using an adaptive system to create phantom sound sources is based on the principal of *Active Noise Control* or *Anti-sound* []. Fig. 1.2 shows the situation. An observer is placed in a room with two closely spaced loudspeakers in-front of him/her (which will be referred to as secondary sound sources). On the position where the phantom sound source should be precieved from, another speaker (which will be referred to as primary sound source or phantom source) is placed producing a certain sound pressure in the eardrums of the observer. The adaptive filters, placed in front of the secondary sources now aims to process the input signal so that the produced sound field interferes in a destructive way with the primary sound field. In the ideal situation when the perceived sound pressure is completely compensated, a phase difference of 180° will exist between the primary sound field and the secondary sound field, hence the observer will experience complete silence (this is known as anti-sound). By terminating the adaption process and removing the primary sound source, the observed sound field

appears to be radiating from the location of the (removed) phantom source. Theoretically this idea seems obvious. Practically however, there are some engineering problems such as measuring the eardrum pressure without changing the sound field, attaining complete cancellation and working with finite accurate equipment. Then of course the question arises if the observer really perceives the phantom source or if there are more complex psycho-acoustic phenomena are involved.
Before practical experiments can be conducted, an adaptive system has to be designed which can be used to control sound fields. For this, the problem is first simplified to a situation where one secondary sound source is used to compensate a primary sound source. When this is accomplished the system can be extended to two or even multiple secondary sound sources.

1.3 Generation of phantom sources using headphones

The last section described a method of creating phantom sources using two secondary loudspeakers placed in front of a listener. The adaptive system used introduces a signal to compensate the primary sound field. The same idea can be applied when instead of secondary sources, headphone are used. Again, the adaptive controllers cancel out the primary sound field, this time using the headphone speakers. The advantage of such a system can be found in the use of low price headphone speakers instead of two more expensive loudspeakers. Also, the relative position from the headphones to the listener is always the same resulting in a non-changing transfer function between secondary sources and ears.

Comment
All experiments described in this report where conducted in an anechoic room at Philips Research and Development in Eindhoven. The assembly programs used for these real time experiments are for internal use only and will not be externally available.

Chapter 2

Introduction to adaptive filters

The principal property of the adaptive system is its time-varying, self-adjusting performance. The need for such an system can be found in situations where fixed design is not realizable due to changing conditions or because the input conditions vary with time or to some extend are unknown. Recent progress in micro-circuit design has resulted in very compact, economical and reliable signal processors for this purpose. For this reason adaptive filters are used in a wide area of applications such as Echo cancelling, Signal estimation Active Noise cancellation and cancelling periodic interference [3, 7, 11] etc..
Before the actual system is modeled a short description will be given of an adaptive system and a widely used and well studied update algorithm. Throughout this report a FIR model will be used to create fixed filter and adaptive filters. This model and other more complex models are described in e.g. [11].

2.1 Adaptive filters

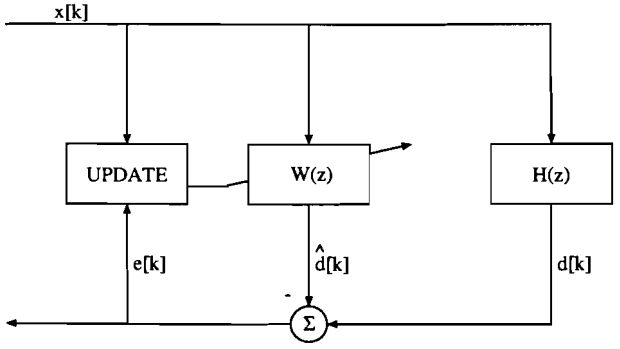

Figure 2.1: Basic adaptive filter situation.

Fig. 2.1 shows a basic layout of an adaptive filter. The filter $W(z)$ aims to compensate the signal $d[k]$ by introducing another signal, namely $\hat{d}[k]$, and so decreasing the error signal $e[k]$. This is done by a controller (in the figure denoted as "UPDATE") which changes the coefficients of the filter so that the error in minimized using a certain criterion. A commonly used criterion is the minimalization of the **M**ean **S**quared **E**rror (**MSE**). Here the average of a sequence of squared errors is taken as measuring quality to be minimized. By squaring the errors and looking at a sequence instead of a single value it is prevented that positive and negative signals cancel out and that at one instant the error is small and at another the error is large. The MSE problem can be stated as the minimalization of

$$J = E\{e^2[k]\}, \tag{2.1}$$

were J is called the loss function or cost function and $E\{\ldots\}$ denotes the mathematical expectation operator.

2.2 LMS algorithm

An algorithm that is often used to minimize the criterion formalized in Eq. (2.1) is the *Widrow-Hoff* or **L**east **M**ean **S**quare algorithm. This recursive gradient descent algorithm is commonly used in adaptive signal processing techniques due to its easy real time implementation possibilities. When using an adaptive filter with an iterative process to update the filter's parameters, one should realize that there are two different ways to create an unstable filter namely:

- Unstablility due to poles outside the unity circle. This is not possible when using a FIR model as a filter, since this model has all the poles in the origin.
- Unstablility due to a non-convergent-update algorithm. When using an iterative update process certain conditions have to be met to ensure stable solution.

In [10] an analysis is given of the properties of this algorithm.
The LMS algorithm, which is used to modify adaptive filter weights, can be expressed as

$$\mathbf{w}[k+1] = \mathbf{w}[k] + \alpha e[k]\mathbf{x}[k]. \tag{2.2}$$

Here α denotes the adaptation constant, which determines the speed and accuracy of convergence, $\mathbf{x}[k]$ is the $(N \times 1)$ vector of the input signal samples in the filter at time k defined as

$$\mathbf{x}[k] = (x[k], x[k-1], \ldots, x[k-N+2], x[k-N+1])^T, \tag{2.3}$$

$\mathbf{w}[k]$ is a $(N \times 1)$ vector of the filter coefficients at time k defined as

$$\mathbf{w}[k] = (w_0[k], w_1[k], \ldots, w_{N-2}[k], w_{N-1}[k])^T \tag{2.4}$$

and N is the length of the adaptive FIR filter. Equating the average value for the coefficient weight vector resolves in optimal solution (also know as the Wiener solution)

$$\mathbf{w}_{opt} = \mathbf{R_x}^{-1} \cdot \mathbf{R_{dx}} \tag{2.5}$$

for $k \rightarrow \infty$. In this equation $\mathbf{R_x}$ is the $(N \times N)$ auto-correlation matrix of the input signal which is defined as

$$\mathbf{R_x} = E\{\mathbf{x}[k]\mathbf{x}^T[k]\} \tag{2.6}$$

and $\mathbf{R_{dx}}$ is the $(N \times 1)$ cross-correlation vector between the input and the desired signal which is defined as

$$\mathbf{R_{dx}} = E\{d[k]\mathbf{x}[k]\}. \tag{2.7}$$

Note
In the ideal situation when $H(z)$ can be completely modelled by $W(z)$, the optimal solution for $W(z)$ will be $W(z)_{opt} = H(z)$ since the signals $d[k]$ and $\hat{d}[k]$ are exactly the same and the error signal $e[k]$ is zero. In practice however this will almost never be the case since $H(z)$ is most likely not of the same model as chosen for $W(z)$.

For the special situation where $x[k]$ is a zero mean white noise signal with variance σ_x^2, the algorithm converges to this optimum solution provided the following condition for α is satisfied:

$$0 < \alpha < \frac{2}{\sigma_x^2}. \tag{2.8}$$

The conclusions form the analysis given in [10] are that when the number of iterations approaches infinity and provided that the adaptation constant lies within the bounds given by Eq. (2.8), the average of the weight vector $\mathbf{w}[k]$ converges to the optimal Wiener solution when using the LMS update algorithm.

Chapter 3

Derivation of model

The adaptive system presented in the previous chapter cannot be applied directly to an active noise control systems (which idea is used to create adaptive phantom sound sources) since there is an acoustic transfer function (referred to as plant) in the "auxiliary path" of adaptive filter (see Fig. 1.2). In this chapter a model will be derived suitable to be used for the creation of phantom sound sources starting with the model illustrated in Chapter 2, assuming linear and time invariant systems. After this, a mathematical description of the signals will be presented and it will be shown that, under certain conditions, the derived algorithm is stable and will converge to the optimum solution.

3.1 Development of filtered-x LMS algorithm

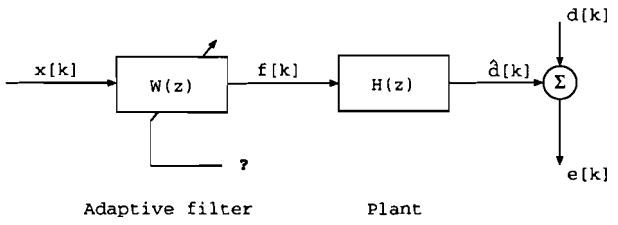

Figure 3.1: Adaptive filter with $H(z)$ in auxiliary path.

The adaptive system illustrated in Fig. 3.1 aims to attenuate the signal $d[k]$ by introducing a cancelling signal $y[k]$. Compared with the simple arrangement for updating the coefficients presented in Chapter 2, the use of an LMS algorithm for this system is more complicated. The difference between the filter output and the desired signal is no longer directly available to update the coefficients, as was the case illustrated in Fig. 2.1. The error signal can now only be observed through the error path $H(z)$. If this signal is to be used directly with in combination with LMS algorithm the adaptive process is almost guaranteed to be unstable (as will be shown in Chapter 4) or find an irrelevant solution. To ensure convergence of the algorithm a

fundamental change has to be made.

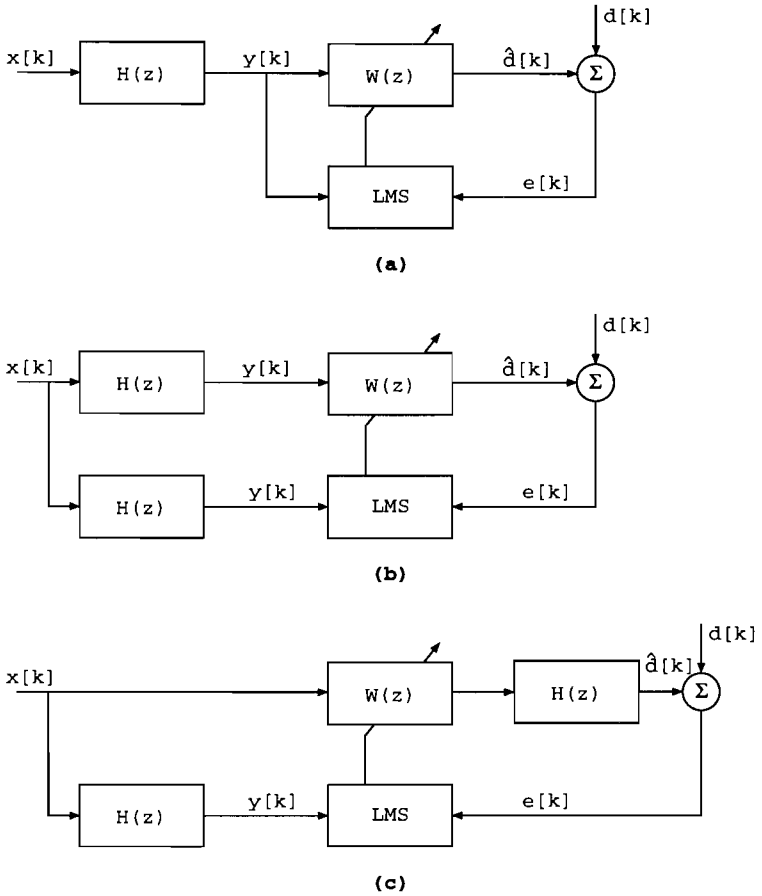

Figure 3.2: Development of the filtered-x LMS algorithm.

For the derivation of a usable model lets first look at Fig 3.2(a) whereupon the LMS algorithm is applied directly. It should be noted that the frequency response of $W(e^{j\theta})$ depends on the frequencies available in the signal $y[k]$ and that the error signal $e[k]$ will only be minimized these frequencies. So, in this case the resulting solution for $W(z)$ using the LMS algorithm depends on the frequency response $H(e^{j\theta})$.

Fig. 3.2(b) shows the same system as before only the adaptive filter input signal and the LMS input signal are now filtered by $H(z)$. This obviously does not change the system since the input signals to the LMS algorithm in both cases are identical at all times.

To go from Fig. 3.2(b) to Fig. 3.2(c) it is assumed that the systems are linear and time invariant. Under these conditions may $H(z)$ be placed in the auxiliary path of $W(z)$ without changing the signal $\hat{d}[k]$. The adaptive filter however, is neither linear nor time invariant. If the adaption of

the coefficients of the adaptive filter takes place on a very slow time-scale it can be assumed that the impulse response is time invariant and linear. $H(z)$ and $W(z)$ are under these conditions commutable without changing the outcome. The now obtained signal $y[k]$ is called **filtered-x** [11] due to the fact that the signal applied to the LMS update module is a filtered version of the input signal $x[k]$.

The derived model demands a copy of the plant to filter the input signal. This, of course is not possible in a practical situation where the plant consists of physical elements such as speakers microphones etc.. It is however, possible to make an estimation of the plants transfer function (which will be referred to as $\hat{H}(z)$) and use this in the filtered-x algorithm in stead of the unavailable plant $H(z)$.

The algorithm just presented is named *filtered-x LMS algorithm* and is first mentioned by Widrow and Stearns [11]. Practical experiments using filtered-x have proven that this system is very robust and they show that the estimated transfer function $\hat{H}(z)$ need not be very precise but only have to lie within certain boundaries of $H(z)$.

To find the boundaries of the used system a mathematical description of the signals has to be derived. At first it is assumed that $\hat{H}(z)$ is a exact copy of $H(z)$ to find the optimal solution for $W(z)$. Then the mean weight convergence of the filtered-x LMS algorithm is calculated to show that under the same conditions as before (that is $\hat{H}(z) = H(z)$) this algorithm converges the optimal solution.

3.2 Mathematical description of filtered-x

Referring to Fig. 3.3, the adaptive control system aims to attenuate an acoustic disturbance by introducing a cancelling signal $y[k]$. Assuming an adaptive FIR filter is used, this signal is derived at any time k by the FIR filtering operation

$$f[k] = \sum_{i=0}^{N-1} x[k-i]w_i[k] = \mathbf{x}[k]^T\mathbf{w}[k], \tag{3.1}$$

where the following vector notation is used for $\mathbf{x}[k]$ and $\mathbf{w}[k]$:

$$\begin{aligned} \mathbf{x}[k] &= (x[k], x[k-1], \ldots, x[k-N+2], x[k-N+1])^T, \\ \mathbf{w}[k] &= (w_0[k], w_1[k], \ldots, w_{N-2}[k], w_{N-1}[k])^T. \end{aligned}$$

Here N is the number of taps in the adaptive filter, $\mathbf{x}[k]$ is the $(N \times 1)$ vector of the input signal samples in the filter at time k and $\mathbf{w}[k]$ is the $(N \times 1)$ vector of the filter coefficients.

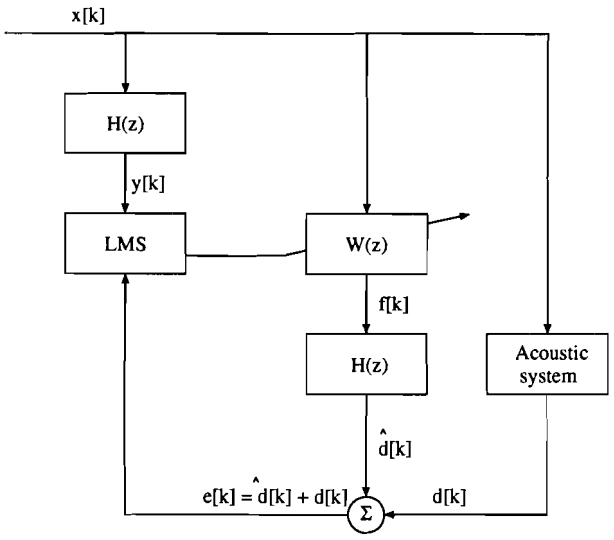

Figure 3.3: Block diagram of an active noise control system using the filtered-x LMS algorithm.

Note
Comparing Fig 3.3 with Fig. 1.2, the transfer function between one secondary loudspeaker and a microphone is here denoted as $H(z)$.

When looking to the normal situation where an adaptive filter is used, the output signal from the filter and the "desired signal" are subtracted to from the error signal $e[k]$. In the situation illustrated if Fig 3.3 the error signal is measured with a microphone. Due to the additive character of this element it sums up the signals $d[k]$ and $\hat{d}[k]$.

3.2.1 Optimal solution

The optimal solution for $W(z)$ can be found by solving Eq. (2.1) which in this case results in

$$J = E\{(d[k] + \hat{d}[k])^2\} = minimal. \tag{3.2}$$

By substituting the relation $\hat{d}[k] = \mathbf{y}^T[k]\mathbf{w} = \mathbf{w}^T\mathbf{y}[k]$ in Eq. (3.2) the mean squared error J becomes:

$$\begin{aligned} J &= E\{(d[k] + \mathbf{w}^T\mathbf{y}[k])(d[k] + \mathbf{y}^T[k]\mathbf{w})\} \\ &= E\{d^2[k]\} + E\{d[k]\mathbf{y}^T[k]\mathbf{w}\} + E\{d[k]\mathbf{w}^T\mathbf{y}[k]\} + E\{\mathbf{w}^T\mathbf{y}[k]\mathbf{y}^T[k]\mathbf{w}\} \\ &= E\{d^2[k]\} + \mathbf{R}_{d\mathbf{y}}^T\mathbf{w} + \mathbf{w}^T\mathbf{R}_{d\mathbf{y}} + \mathbf{w}^T\mathbf{R}_{\mathbf{y}}\mathbf{w} \end{aligned} \tag{3.3}$$

where $\mathbf{R}_{d\mathbf{y}}$ is the $(N \times 1)$ vector of the cross-correlation between $d[k]$ and $\mathbf{y}[k]$ and $\mathbf{R}_{\mathbf{y}}$ is the $N \times N$ auto-correlation matrix defined as

$$\begin{aligned} \mathbf{R}_{d\mathbf{y}} &= E\{d[k]\mathbf{y}[k]\} \\ \mathbf{R}_{\mathbf{y}} &= E\{\mathbf{y}[k]\mathbf{y}^T[k]\}. \end{aligned}$$

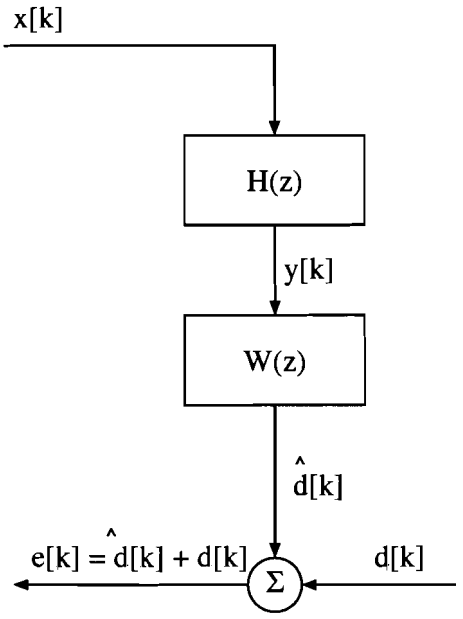

Figure 3.4: Block diagram where $W(z)$ is the optimal solution.

Eq. (3.3) can be minimized by taking the derivative of J with respect to the coefficient w_i and solving this for zero solution. This resolves in N linear equation of the form:

$$\frac{\delta J}{\delta w_i} = 0. \tag{3.4}$$

Hence the optimal solution, $\mathbf{w}_{opt}$, can be found by solving the Eq. (3.4). This results in

$$\frac{\delta J}{\delta \mathbf{w}} = 2\mathbf{R}_{\mathbf{dy}} + 2\mathbf{R}_{\mathbf{y}}\mathbf{w}_{opt} = 0 \tag{3.5}$$

or

$$\mathbf{w}_{opt} = -\mathbf{R}_{\mathbf{y}}{}^{-1}\mathbf{R}_{\mathbf{dy}}. \tag{3.6}$$

3.2.2 Convergence of filtered-x LMS algorithm

To find the optimum solution for $W(z)$ for the case depicted in Fig. 3.3 the block diagram is drawn up slightly different in Fig. 3.5 which is allowed since the adaptive filter and the plant are assumed to be linear and time invariant (same conditions as before). To see the average weight convergence properties of the filtered-x update algorithm, it is assumed that an exact copy of the plant is available and is placed in front of the LMS update unit as depicted in Fig. 3.5.

The filtered-x LMS algorithm, which is used to modify adaptive filter weights can be expressed as

$$\mathbf{w}[k+1] = \mathbf{w}[k] - \alpha e[k]\mathbf{y}[k]. \tag{3.7}$$

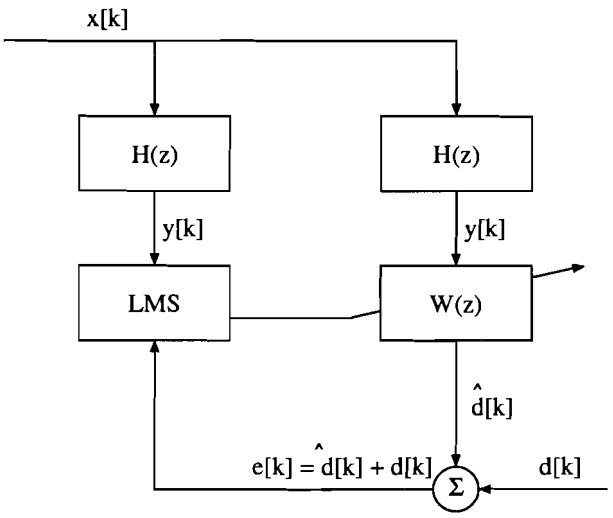

Figure 3.5: Equivalent block diagram. Here an exact copy of the plant is available and is placed in front of the LMS update unit.

To determine the average weight solution the expectation operator is applied on Eq. (3.7) which results in

$$\begin{aligned} E\{\mathbf{w}[k+1]\} &= E\{\mathbf{w}[k]\} - \alpha E\{e[k]\mathbf{y}[k]\}, \\ &= E\{\mathbf{w}[k]\} - \alpha E\{(d[k] + \hat{d}[k])\mathbf{y}[k]\}, \\ &= E\{\mathbf{w}[k]\} - \alpha E\{d[k]\mathbf{y}[k]\} - \alpha E\{\hat{d}[k]\mathbf{y}[k]\}, \end{aligned} \tag{3.8}$$

using the relation $\hat{d}[k] = \mathbf{y}^T[k]\mathbf{w}[k]$ leads to

$$\begin{aligned} E\{\mathbf{w}[k+1]\} &= E\{\mathbf{w}[k]\} - \alpha E\{d[k]\mathbf{y}[k]\} - \alpha E\{\mathbf{y}[k]\mathbf{y}^T[k]\mathbf{w}[k]\} \\ &= E\{\mathbf{w}[k]\} - \alpha \mathbf{R}_{d\mathbf{y}} - \alpha \mathbf{R}_{\mathbf{y}} E\{\mathbf{w}[k]\} \\ &= (I - \alpha \mathbf{R}_{\mathbf{y}}) E\{\mathbf{w}[k]\} - \alpha \mathbf{R}_{d\mathbf{y}}. \end{aligned} \tag{3.9}$$

where $\mathbf{I}$ is the $N \times N$ unity matrix. It is assumed here that due to a much slower variation of $\mathbf{w}[k]$ in comparison to the variation $\mathbf{y}[k]$ they may be separated under $E\{\ldots\}$.
Equating the last equation comes to

$$\begin{aligned} E\{\mathbf{w}[k+1]\} &= (I - \alpha \mathbf{R}_{\mathbf{y}})^{k+1} E\{\mathbf{w}[0]\} - \alpha \mathbf{R}_{d\mathbf{y}} \sum_{n=0}^{k} (I - \alpha \mathbf{R}_{\mathbf{y}})^n \\ &= (I - \alpha \mathbf{R}_{\mathbf{y}})^{k+1} \mathbf{w}[0] - \alpha \mathbf{R}_{d\mathbf{y}} \sum_{n=0}^{k} (I - \alpha \mathbf{R}_{\mathbf{y}})^n \end{aligned} \tag{3.10}$$

When $k \to \infty$ is used in Eq. (3.10), the resulting solution will give the value to which the adaptive weight will converge to (Eq. (3.11)) and what the boundaries for α will be so the algorithm is stable (Eq. (3.12)).

$$\mathbf{w}_\infty = -\mathbf{R}_{\mathbf{y}}{}^{-1} \mathbf{R}_{d\mathbf{y}} \tag{3.11}$$

$$|I - \alpha \mathbf{R_y}| < 1 \tag{3.12}$$

As commonly done in a stability analysis of the LMS algorithm, Eq. (3.12) can be decoupled using a orthonormal transformation due to the symmetric nature of the matrix $\mathbf{R_y}$. The bounds for stable operation for the filtered-x LMS algorithm is now found to be the same as the bounds found for the normal LMS algorithm

$$0 < \alpha < \frac{2}{\lambda_{max}} \tag{3.13}$$

where λ_{max} is the maximum eigenvalue of $\mathbf{R_y}$.

3.3 Conclusions

From the analysis above can be concluded that, when an exact copy of the plant is placed in front of the LMS update unit, the filtered-x algorithm will converge (in average) to the optimal solution, $\mathbf{w}_{opt}$, if the adaptation constant α is set within the bounds given by Eq. (3.12) and (3.13). It can be said that the bounds of stability are determined by the input signal used and the plants transfer function.

Chapter 4

Effect of estimated transfer function errors

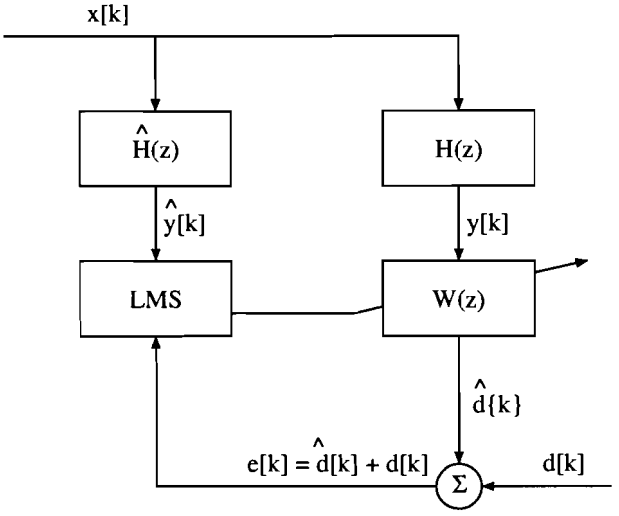

Figure 4.1: An estimation of the plant, $\hat{H}(z)$, is made and placed in front of the the LMS update unit.

The practical implementation of the filtered-x LMS algorithm includes an copy of the plants transfer function as shown in Chapter 3. In general, an exact copy will not be available and an estimation of the plant is used instead. In [11] it was mentioned that the estimation need not be very precise, not saying exactly what "not very precise" means.
Fig. 4.1 shows the situation where the unavailable plant, $H(z)$ is substituted by an estimation version $\hat{H}(z)$. Since this estimation is not an exact copy of $H(z)$, errors will exist resulting in a difference between the signals $y[k]$ and $\hat{y}[k]$.
In [2, 7, 9] an analysis is given on the behavior of the filtered-x algorithm when an error exists between plant and the estimation of the plant. In this chapter the influence of the transfer function estimation errors on the systems stability bounds is examined to give more insight into the problems

that exist when using the filtered-x LMS algorithm. The one chosen here will be the simple case of a two-tap adaptive filter being used to control a sinusoidal primary disturbance.

4.1 Effect of transfer function estimation errors

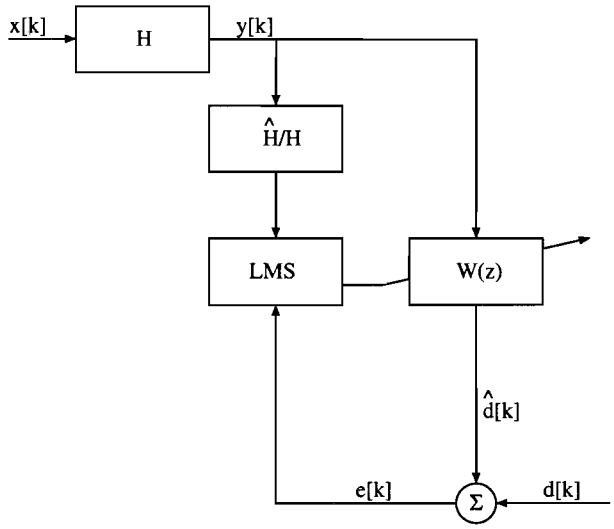

Figure 4.2: Plants transfer function and adaptive filter change place.

Referring to Fig. 4.2, the lumped transfer function in front of the LMS algorithm now represents the total error made between the real plants transfer function $H(\omega)$ and the estimation of the plant transfer function $\hat{H}(\omega)$. Suppose that the input signal for the adaptive filter ($y[k]$) is a pure sine wave with frequency ω_y, then this lumped transfer function can be thought of as a simple gain and phase change and hence can be described by a (complex) scalar h which can be calculated with:

$$\begin{aligned} \mathsf{h} &= \frac{\hat{H}(\omega_y)}{H(\omega_y)} \\ &= \frac{|\hat{H}|e^{j\hat{\phi}}}{|H|e^{j\phi}} \\ &= \frac{|\hat{H}|}{|H|}e^{j(\hat{\phi}-\phi)} \\ &= |H_e|e^{j\phi_e}, \end{aligned} \tag{4.1}$$

where $|H|$, ϕ, $|\hat{H}|$ and $\hat{\phi}$ are respectively the gain and phase of the plant and the gain and phase of the estimation of the plant for the frequency ω_y. $|H_e|$ and ϕ_e represents the magnitude and the phase error made between the real plant and the estimation of the plant. To study the effect this has on the systems bounds of stability the mean weight convergence is calculated when the filtered-x algorithm is used to update the coefficients.

4.1.1 Theoretical calculations

The input signal used for the system shown in Fig. 4.2 is a single frequency signal given by

$$y[k] = A_y \sin(\omega_y T k), \tag{4.2}$$

where $1/T$ is the sample frequency.
Since the filtered-x LMS algorithm is used the update equation is given by

$$\mathbf{w}[k+1] = \mathbf{w}[k] - \alpha e[k] \mathbf{h} \mathbf{y}[k], \tag{4.3}$$

where $\mathbf{w}[k]$ a (2×1) [1] vector is of the adaptive filter weights, $\mathbf{y}[k]$ is a (2×1) vector defined as

$$\mathbf{y}^T[k] = (y[k], y[k-1]) \tag{4.4}$$

and

$$e[k] = d[k] + \hat{d}[k] = d[k] + \mathbf{y}^T[k]\mathbf{w}[k]. \tag{4.5}$$

To see the mean weight convergence of the filtered-x algorithm , Eq. (4.3) and Eq. (4.5) are combined and the expectation operator is applied. Assuming that the input vector $\mathbf{y}[k]$ and the weight vector $\mathbf{w}[k]$ may be separated under $E\{\ldots\}$ this results in:

$$\begin{aligned} E\{\mathbf{w}[k+1]\} &= E\{\mathbf{w}[k]\} - \alpha \mathbf{h} E\{\mathbf{y}[k]d[k] + \mathbf{y}[k]\mathbf{y}^T[k]\mathbf{w}[k]\} \\ &= E\{\mathbf{w}[k]\} - \alpha \mathbf{h} \mathbf{R}_{\mathbf{dy}} - \alpha \mathbf{h} \mathbf{R}_{\mathbf{y}} E\{\mathbf{w}[k]\} \\ &= (I - \alpha \mathbf{h} \mathbf{R}_{\mathbf{y}})\, E\{\mathbf{w}[k]\} - \alpha \mathbf{h} \mathbf{R}_{\mathbf{dy}}. \end{aligned} \tag{4.6}$$

Here $\mathbf{R}_{\mathbf{dy}}$ is the correlation function between the input signal $y[k]$ and the desired signal $d[k]$ and $\mathbf{R}_{\mathbf{y}}$ is autocorrelation function matrix which, in this case, is given by the

$$\begin{aligned} \mathbf{R}_{\mathbf{y}} &= E\{\begin{pmatrix} y[k] \\ y[k-1] \end{pmatrix} (y[k], y[k-1])\} \\ &= \frac{A_y^2}{2} \begin{pmatrix} 1 & \cos(\omega_y T) \\ \cos(\omega_y T) & 1 \end{pmatrix}. \end{aligned} \tag{4.7}$$

Since the input autocorrelation function matrix, $\mathbf{R}_{\mathbf{y}}$, is symmetric, it can be diagonalized using

$$\mathbf{Q}^{-1} \mathbf{R}_{\mathbf{y}} \mathbf{Q} = \mathbf{\Lambda}, \tag{4.8}$$

where $\mathbf{Q}$ is the orthonormal matrix (the matrix of eigenvectors) and $\mathbf{\Lambda}$ is the diagonal matrix of eigenvalues of $\mathbf{R}_{\mathbf{y}}$. Calculating $\mathbf{Q}$ and $\mathbf{\Lambda}$ of $\mathbf{R}_{\mathbf{y}}$ results in:

$$\begin{aligned} \mathbf{Q} &= \frac{1}{\sqrt{2}} \begin{pmatrix} -1 & 1 \\ 1 & 1 \end{pmatrix}, \\ \mathbf{\Lambda} &= \frac{A_y^2}{2} \begin{pmatrix} 1 - \cos(\omega_y T) & 0 \\ 0 & 1 + \cos(\omega_y T) \end{pmatrix}. \end{aligned} \tag{4.9}$$

[1] The richness of a signal is determined by the number of frequencies is consists of. In general it can be sad that to estimate $2n$ parameters (weights), the input signal should at-least contain n different frequencies. For the single frequency input case, 2 filter weights can be estimated.

To decouple the elements of $E\{\mathbf{w}[k+1]\}$ in Eq. (4.6) both sides are multiplied by $\mathbf{Q}^{-1}$ and rearranged as follows:

$$\begin{aligned}
\mathbf{Q}^{-1}E\{\mathbf{w}[k+1]\} &= \mathbf{Q}^{-1}E\{\mathbf{w}[k]\} - \alpha\mathsf{h}\mathbf{Q}^{-1}\mathbf{R}_{dy} \\
&\quad -\alpha\mathsf{h}\mathbf{Q}^{-1}\mathbf{R}_{\mathbf{y}}\mathbf{Q}\mathbf{Q}^{-1}E\{\mathbf{w}[k]\} \\
E\{\mathbf{w}'[k+1]\} &= E\{\mathbf{w}'[k]\} - \alpha\mathsf{h}\mathbf{R}'_{dy} - \alpha\mathsf{h}\mathbf{\Lambda}E\{\mathbf{w}'[k]\} \\
&= (I - \alpha\mathsf{h}\mathbf{\Lambda})\, E\{\mathbf{w}'[k]\} - \alpha\mathsf{h}\mathbf{R}'_{dy} \\
&= (I - \alpha\mathsf{h}\mathbf{\Lambda})^{k+1}\, E\{\mathbf{w}'[0]\} \\
&\quad -\alpha\mathsf{h}\mathbf{R}'_{dy}\sum_{n=0}^{k}(I - \alpha\mathsf{h}\mathbf{\Lambda})^{n}\,. \qquad (4.10)
\end{aligned}$$

Here, $E\{\mathbf{w}'[k]\}$ and $\mathbf{R}'_{dy}$ are defined as

$$\begin{aligned}
E\{\mathbf{w}'[k]\} &= \mathbf{Q}^{-1}E\{\mathbf{w}[k]\} \\
\mathbf{R}'_{dy} &= \mathbf{Q}^{-1}\mathbf{R}_{dy}
\end{aligned}$$

It follows from Eq. (4.10) that the average behavior of the vector $\mathbf{w}'[k]$ and hence $\mathbf{w}[k]$ converges to the optimal solution, as $k \to \infty$, provided the following condition is satisfied:

$$|I - \alpha\mathsf{h}\mathbf{\Lambda}| < 1, \qquad (4.11)$$

or

$$|1 - \alpha\mathsf{h}\lambda_{\mathbf{i}}| < 1, \qquad (4.12)$$

where i is 1 or 2.
The last step that has to be taken to find the bounds of average stability of the filtered-x algorithm is splitting up h into it's real and imaginary parts and solving Eq. (4.12). This works out to be

$$\alpha < \frac{2h_R}{|H_e|^2\lambda_i} \qquad (4.13)$$

or

$$\alpha < \frac{2}{\lambda_i}\frac{\cos(\phi_e)}{|H_e|} \qquad (4.14)$$

where h_R is the real part of h, h_I is the imaginary part of h and ϕ_e is defined as $\tan^{-1}(h_I/h_R)$.
Thus, the bounds placed on α for convergence are

$$0 < \alpha < \frac{2}{\lambda_i}\frac{\cos(\phi_e)}{|H_e|}. \qquad (4.15)$$

As can be seen from this last equation, when there is no estimation error and so when $\phi_e = 0$ and $|H_e| = 1$, the bound for α are the same as would be found when using normal LMS with no transfer function in the auxiliary path.
However, if there is an error in the estimated transfer function the bounds differ from the normal case and the problem can be divided into two parts namely:

- An error made in the amplitude characteristic of the estimated transfer function. This means that$|H_e| \neq 1$.
- An error made in the phase characteristic of the estimated transfer function in which case $\phi_e \neq 0°$.

Error in magnitude estimation

Since α is proportional to the reverse of this error, as can be seen in Eq. (4.15), errors in the estimation of the amplitude only effects the upper bound of α for which the algorithm converges due to the changing of $|H_e|$. This however, does not have to be a problem since it will always be within certain limits. The adaptive constant α can always be compensated so the algorithm will converge to it's optimum solution.

Error in phase estimation

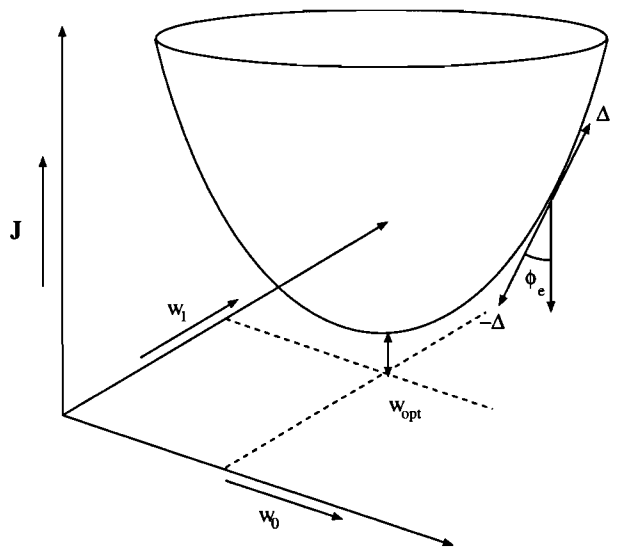

Figure 4.3: J as function of the adaptive weights w_0 and w_1.

Fig. 4.3 shows a graph of the mean-squared error [2] J as function of the adaptive weights w_0 and w_1. Due to the parabolic nature of $J = f(\mathbf{w})$ the gradient vector $\nabla = \delta J/\delta \mathbf{w}$ always points away from the minimum mean-squared error J_{min}. The LMS algorithm is based on the *steepest-descent* algorithm which means that the adaptive weights are updated in the opposite direction of the gradient. If a phase error occurs between the input of the update mechanism (in this case ϕ_e) and the input of the adaptive filter ($y[k]$) the updating will not go exactly in the opposite direction of the gradient vector but it will make a slight angle with this maximum. As this angle becomes larger the speed of convergence slows down due to a small resultant in the direction of the gradient. If the phase difference reaches 90°

[2]The mean-squared error is defined as $E\{e^2[k]\}$.

or more the weights of the filter will not converge to the optimum anymore and will even become unstable.
Looking at the parabolic error surface of Fig. 4.3 is only one way to show that the algorithm becomes unstable when a too large an error is made in the phase estimation transfer function. Another way is looking at the convergence region for α given in Eq. (4.15). This equation shows that when $|\phi_e|$ exceeds 90° the region of convergence is non existing and that there is no α for which the filter converges.

This analysis has shown that under certain conditions the filtered-x algorithm becomes unstable and that these conditions are mainly determined by the error made in the phase estimation of the plants transfer function. When the phase error exceeds the 90° limit the algorithm is unstable for every value of α so it can be said that for the algorithm to converge to the optimal solution the next two conditions have to be met:

- $-90° < \phi_e < 90°$
- $\alpha < \frac{2}{\lambda_i} \frac{\cos(\phi_e)}{|H_e|}$

4.1.2 Simulation of phase error

In the preceding sections it was shown that for certain conditions the filtered-x algorithm would become unstable. In this section a simulation is made using the program Matlab. The aim of this simulation is to show that the found limitations of the filtered-x algorithm with respect to the allowed phase error are real and that it is something to take into account when using this algorithm.

Referring to Fig. 4.2, the desired signal $d[k]$ is derived from $y[k]$ using a 2 coefficient FIR with z-transform function

$$Q(z) = -0.5 - 0.5z^{-1} \tag{4.16}$$

leaving the optimal solution for $\mathbf{w}$ to be

$$\mathbf{w}^T = (0.5, 0.5). \tag{4.17}$$

The lumped transfer function $\hat{H}/H$ will also be modelled by a 2 coefficients FIR filter with z-transform function

$$H_e(z) = h_0 + h_1 z^{-1} \tag{4.18}$$

where h_0 and h_1 are parameters that can be changed so a certain phase and/or magnitude error will occur. To calculate this phase and magnitude error, $H_e(z)$ should be evaluated on the unit circle $|z| = 1$. This resolves in

$$\begin{aligned} H_e\left(e^{j\theta}\right) &= h_0 + h_1 e^{-j\theta} \\ &= h_0 + h_1 \cos(\theta) - j h_1 \sin(\theta). \end{aligned} \tag{4.19}$$

Here θ represents the relative frequency which is defined as

$$\theta = \omega_y T = \frac{2\pi f_y}{f_{sample}}. \tag{4.20}$$

To find the actual phase and magnitude error of H_e the absolute value and the argument of Eq. (4.19) have to be calculated for the frequency of $y[k]$. This work out to be

$$|H_e| = \sqrt{h_0^2 + h_1^2 + 2h_0 h_1 \cos(\theta)}, \tag{4.21}$$

and

$$arg\,(H_e) = \phi_e = \tan^{-1}\left(\frac{-h_1 \sin(\theta)}{h_0 + h_1 \cos(\theta)}\right). \tag{4.22}$$

By making the sample frequency 4 times bigger than the input signal frequency ($fs = 4 \cdot f_y$) and so by making $\theta = \frac{\pi}{2}$ the phase and magnitude error are simplified to:

$$|H_e| = \sqrt{h_0^2 + h_1^2}, \tag{4.23}$$

and

$$arg\,(H_e) = \tan^{-1}\left(\frac{-h_1}{h_0}\right). \tag{4.24}$$

For this simulation a constant magnitude error of $|H_e| = 1$ is opholded to leave a simple relation between the coefficients of the lumped error filter and the phase error ϕ_e. This relation is given by

$$\begin{aligned} h_0 &= \cos(\phi_e), \\ h_1 &= -\sin(\phi_e). \end{aligned} \tag{4.25}$$

One of the parameters that determines the boundaries of α is the maximum eigenvalue of the auto-correlation matrix $\mathbf{R_y}$ as can be seen in Eq. (4.15). The maximum eigenvalue is a function of the relative frequency θ and is for the chosen input frequency $\lambda_{max} = 1/2$. So for the chosen frequency the boundaries for stability on α are simplified to

$$0 < \alpha < 4\cos(\phi_e), \tag{4.26}$$

as shown in Fig. 4.4. In this simulation $\alpha = 0.1$ is chosen and every time the

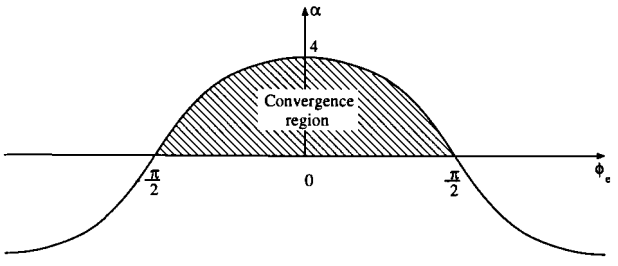

Figure 4.4: α as function of the phase error ϕ_e.

phase error is enlarged by 15° until it reaches 90°. Then another single step

is made where the phase error is made 91° in which case it falls outside the convergence region. Fig. 4.5 shows these results where on the $x - axis$ the phase error, on the $y - axis$ the number of iterations and on the $z - axis$ the quadratic error $e^2[k]$ is plotted.

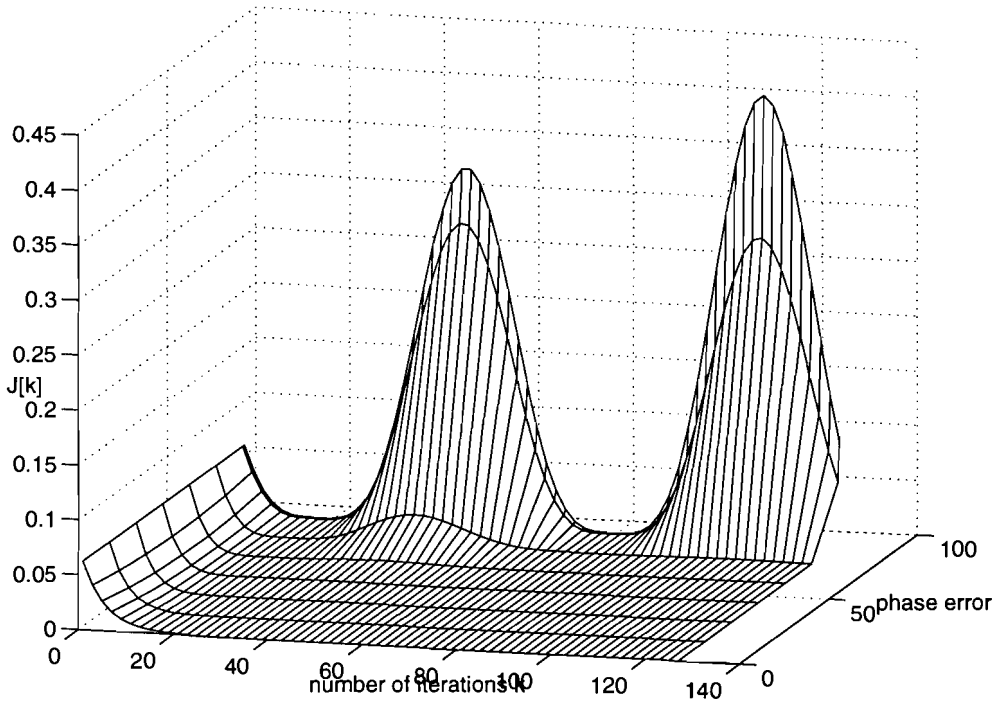

Figure 4.5: Surface plot of the quadratic error $J[k] = e^2[k]$ as a function of the number of iterations and the phase error.

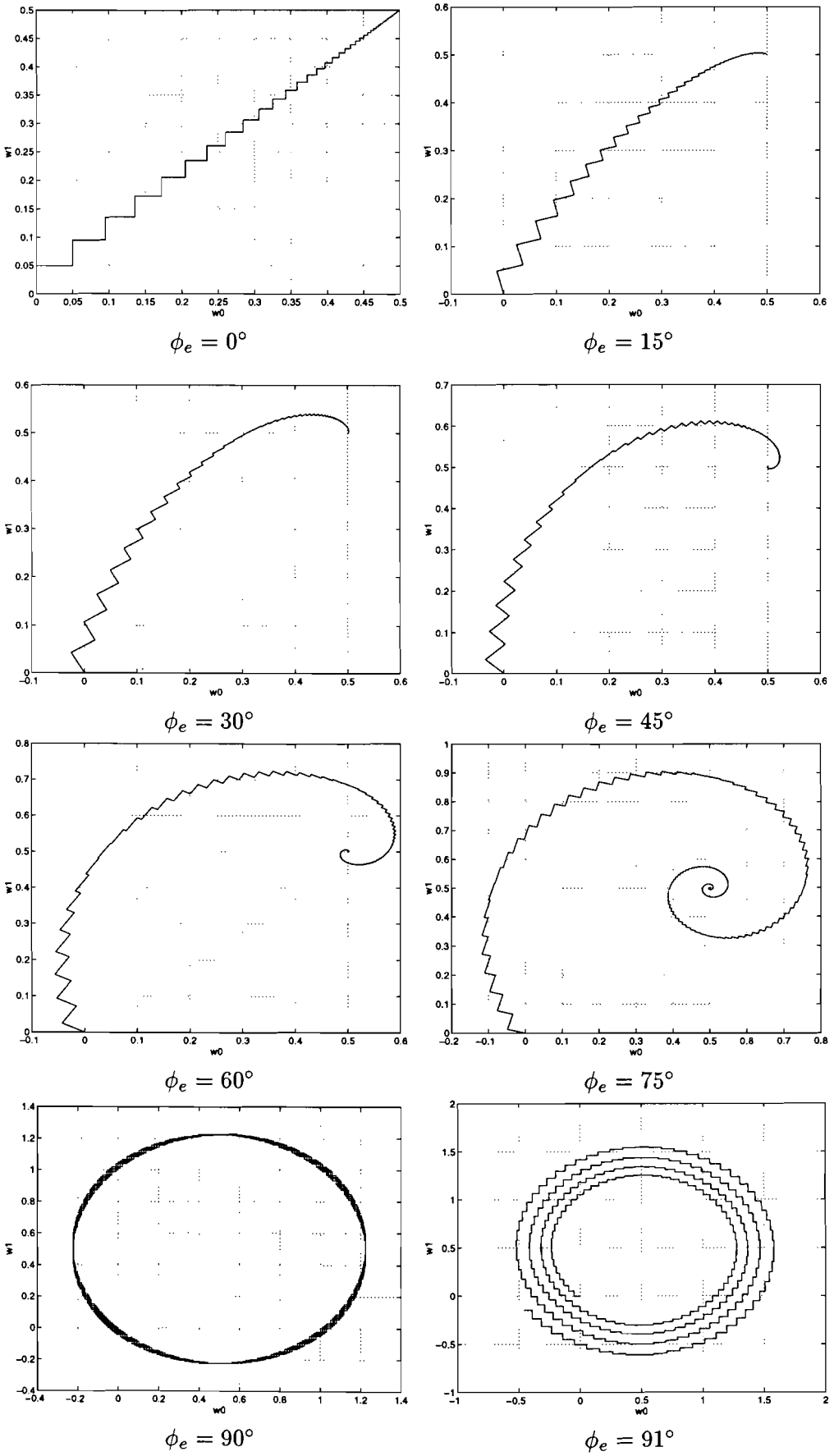

$\phi_e = 0°$ $\phi_e = 15°$

$\phi_e = 30°$ $\phi_e = 45°$

$\phi_e = 60°$ $\phi_e = 75°$

$\phi_e = 90°$ $\phi_e = 91°$

Figure 4.6: w_1 versus w_0 with changing phase error ϕ_e.

Fig. 4.6 shows the iterative weight change of w0 and w1 when the phase error changes. It can be seen from these figures that when there is no phase error, the weights go in a almost strait line to the optimum solution. As the phase error becomes lager the number of iteration needed to reach this optimum increases and in the last the optimum is never reached. Table 4.1 gives the number of iterations needed for the algorithm to converge (within 1 %) to the optimal solution when the phase error changes.

ϕ_e	number of iterations
0°	119
15°	126
30°	147
45°	173
60°	247
75°	482
90°	never
91°	never

Table 4.1: Number of iteration needed for the weight to converge within 0.1 of the optimum value.

4.2 Conclusions

Errors in the estimation of the plants transfer function needed for the filtered-x to be used in an active control system influence the stability of the algorithm. The errors made between the real plant and the estimation can be split up into two separate parts namely:

- Errors made in the magnitude. This error will alter the maximum stable value of the convergence coefficient α through an inverse proportional relation. It is, however possible to compensate this error by reducing α.
- Errors made in the phase. The phase error may not exceed $\pm 90°$ for the algorithm to be stable.

From the simulations outlined in this chapter it can be concluded that when the phase error becomes larger, but stays within the $\pm 90°$ phase error limit, the speed of convergence becomes slower and more iterations are needed to reach the optimal solution.

Chapter 5

Practical implementation of filtered-x algorithm

The creation of phantom sound sources with adaptive filters is based on the idea of active noise control where a primary sound source is compensated by other (one or more secondary) sound source(s). In Chapter 3, the filtered-x algorithm was derived for this purpose. An implementation of this algorithm requires a copy of the plants transfer function in front of the LMS update unit. In a practical situation this transfer function is unavailable and instead an estimation is used. Chapter 4 dealt with the convergence properties of the filtered-x algorithm when an error is made between this estimation and the real plant.
In this chapter a scheme will be presented where prior to control of sound an estimation of the plant is made and placed in front of the LMS update unit.

5.1 Initialization of filtered-x algorithm

A possible scheme to use the filtered-x method is shown in Fig. 5.1 in which two separate adaptive processes are used. Prior to control, $AFIR1$ produces a direct estimation of the plants transfer function. After convergence, the weights of $\hat{H}(z)$ are copied to the place of the unavailable plant to generate the reference signal $\hat{y}[k]$. After this initialization step, $AFIR2$ is ready to be used as an active noise controller.

The modelling of the acoustical system $H(z)$, as shown in Fig. 5.1, is not very efficient since the delay introduced, due to the distance between the speaker and the microphone, is also included. The resulting transfer function will start with a number of zeros leaving less weights to model the more relevant part of $H(z)$. It is however, possible to overcome this problem by placing a delay-line in front of the adaptive system as shown in Fig. 5.2 where part of the delay is compensated by $z^{-\Delta}$. It should be noted that the length of the delay-line must be carefully selected. If Δ is chosen to be big, the first part of $H(z)$ can not be modeled and a lot important information is lost. If

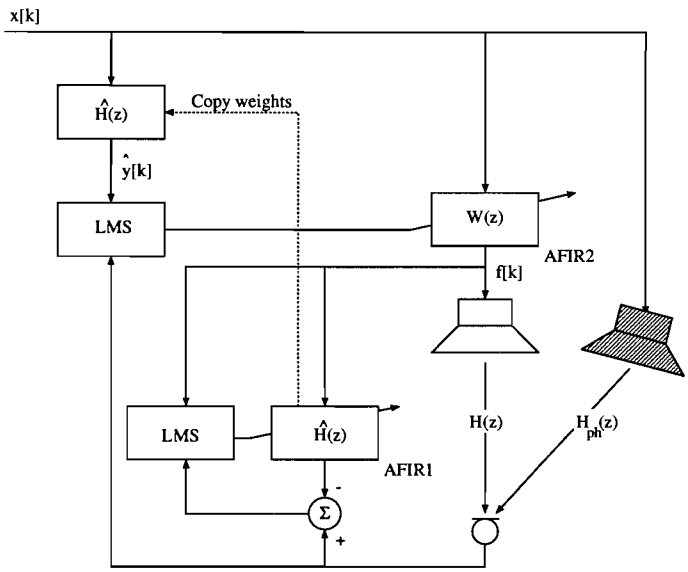

Figure 5.1: A practical implementation of the filtered-x algorithm.

however, Δ is too small, the adaptive filter $W(z)$ will emulate a useless delay.

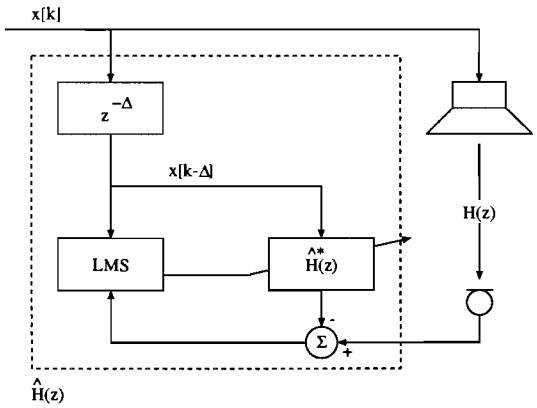

Figure 5.2: The acoustical delay is partly compensated by $z^{-\Delta}$.

One way of measuring the acoustical delay is by making a correlation analysis between the the speaker (input) signal and the microphone (output) signal. In practice however, it is easier to make an estimation by calculating the time acoustical delay relative to the sample frequency using

$$\Delta = \frac{f_s L_a}{c} \tag{5.1}$$

where f_s is the sample frequency of the digital signal processing system, c is the speed of sound in air, L_a is the distance between the speaker and the microphone and Δ is the length of the delay-line (in samples).

The delay-line (denoted in the figure as $z^{-\Delta}$) and adaptive filter (denoted in the figure as $\hat{H}^*(z)$) together form $\hat{H}(z)$ and can be used in the filtered-x algorithm in place of the unavailable plant.

Chapter 6

Single point cancellation

In this chapter an experiment will be described, utilizing a single point active noise canceller. The aim of this experiment is to study the concept of using an adaptive system together with the filtered-x algorithm before it is used to create phantom sources. The speed of convergence is not in quest here so the measurements will be done after the result is stabilized. The only goals of this experiment are to see if the algorithm works and what kind of reduction can be made using this algorithm.
The experiments were carried out in a anechoic room to minimize the effect of reflection, revibration and other room interferences. Here a microphone and two loudspeakers were installed. One loudspeaker functioned as primary sound source to emit a sound field in the enclosure. The other loudspeaker was used to generate a secondary sound field to reduce the sound pressure in the vicinity of the microphone. The type of primary noise used is band limited white noise.
In this experiment the power of the microphone signal is measured before and after cancellation using a HP3562A dynamic signal analyzer and placed in one figure. The results presented are the average of 50 measurements to improve the signal to noise ratio. Since the input signal is band limited, only the relevant part of this power spectrum will be shown.

6.1 Experiments

6.1.1 Conditions

In the practical system illustrated in Fig. 6.1, the adaptive filter $W(z)$ is used to operate on the input signal $x[k]$ to drive the secondary source in such a way the microphone signal $e[k]$ is minimized. The implementation for this experiment was done on a single DSP56002 digital signal processor from Motorola [1] operating at 70 MHz. The output signal of the adaptive filter was converted using 16 bits Digital to Analog converters. This signal was applied to an amplifier to drive the secondary loudspeaker. The error signal $e[k]$ and the input signal $x[k]$ where sampled using 16 bits Analog to

[1] For hardware specifications refer to [6]

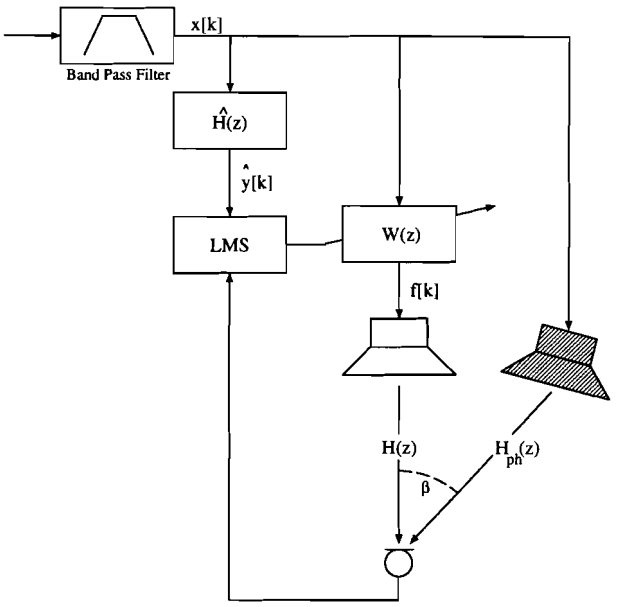

Figure 6.1: Practical experiment with single point cancellation

Digital Converters at a sample rate of 11025 Hz. The input signal used was band-limited white noise with a bandwidth reaching from 200 Hz to 5000 Hz.

Note
The loudspeakers used for this experiment had a poor response for frequencies below 200 Hz. Further, to leave some margin between the Nuquist frequency and the highest input frequency the white noise was limited to 5000 Hz.

Prior to control, during an initialization phase, the transfer function between the secondary source and the microphone was estimated using an adaptive FIR filter with 256 taps. This filter was subsequently used to generate the reference signal $\hat{y}[k]$ (see Fig. 6.1). The adaptive cancelling filter $W(z)$ was modelled using again a FIR filter of 256 taps.
The loudspeaker used as the secondary sound source was mounted at 182 cm from the top of the microphone. The second loudspeaker serving as primary sound source was mounted on a movable stand. While maintaining a constant distance of 220 cm between this loudspeaker and the microphone, the angle β was changed and the microphone power was measured.

The digital signal processor used had to perform each sample period the next tasks:

- Calculating the filtered-x signal

$$\hat{y}[k] = \sum_{n=0}^{255} x[k-n]\hat{h}_n,$$

- Calculating the secondary source signal

$$f[k] = \sum_{n=0}^{255} x[k-n]w_n[k],$$

- Updating the adaptive filter coefficients using

$$\mathbf{w}[k+1] = \mathbf{w}[k] - \alpha e[k]\hat{\mathbf{y}}[k].$$

Here $\hat{h}_n$ is the n^{th} coefficient of the impulse response of the estimated plant transfer function and $w_n[k]$ is the n^{th} coefficient of the adaptive filter at time instant k.

Comments
In an optimal situation where the primary field is completely compensated by the secondary field, the transfer function of the adaptive filter would be

$$W(z) = -H_{ph}(z)/H(z). \tag{6.1}$$

This would be the best result possible since for this case the error signal $e[k]$ would be zero. If the loudspeakers used for the primary source and the secondary source are exactly the same and if the the microphone used was infinitely small, the optimal solution for the adaptive filter $W(z)$ would only be a time-delay, compensating the difference in distance between the two loudspeakers. This could obviously only be accomplished if the distance from the microphone to the primary loudspeaker is bigger than the distance from microphone to the secondary loudspeaker since then the adaptive filter has to be causal. Practically these conditions for exact cancelling will not hold due to finite dimensions of the microphone and the loudspeakers will not be exactly the same. It is however, an idea to bear in mind when doing practical experiments since this simplified theory says that the primary source should not be positioned closer to the microphone than the secondary source. The experiment was for this reason conducted using a secondary sound source at 182 cm and a primary sound source at 220 cm.
For the initial setup an angle $\beta = 30°$ is opholded. The power of the microphone is now measured with only the primary source radiating. Then the active noise canceller is switched on and, after stabilization, the microphone power is measured again. These two results are placed in a single figure for an easy comparison. Then the angle β in increased by 30° while maintaining a distance between the primary source and the microphone of 220 cm. This is repeated until the angle is 180°.

6.1.2 Results

Fig. 6.2 and Fig. 6.3 show the results from the experiment with on the left side the power of the microphone before (solid line) and after cancellation (dashed line) with increasing β. The right side of these figures show the impulse response of the adaptive filter needed to accomplish the cancellation. It follows from these results that the self-tuning ANC algorithm can perform well and is capable of providing a large reduction of signal power.

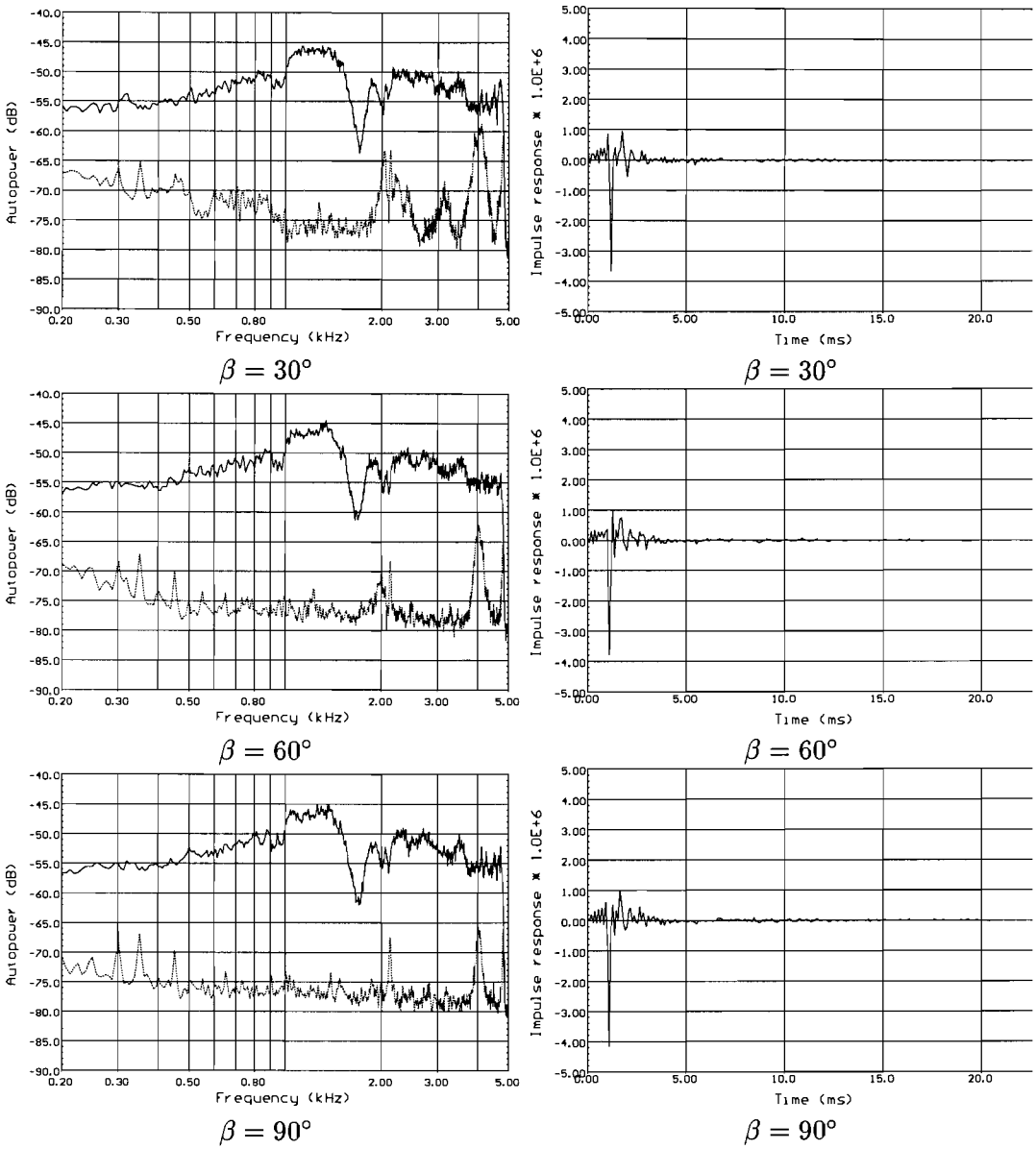

Figure 6.2: Results from measurements using an adaptive noise canceller. The pictures on the left side show the microphone power before (solid) and after cancellation (dashed). The pictures on the right side show the adaptive filter weights.

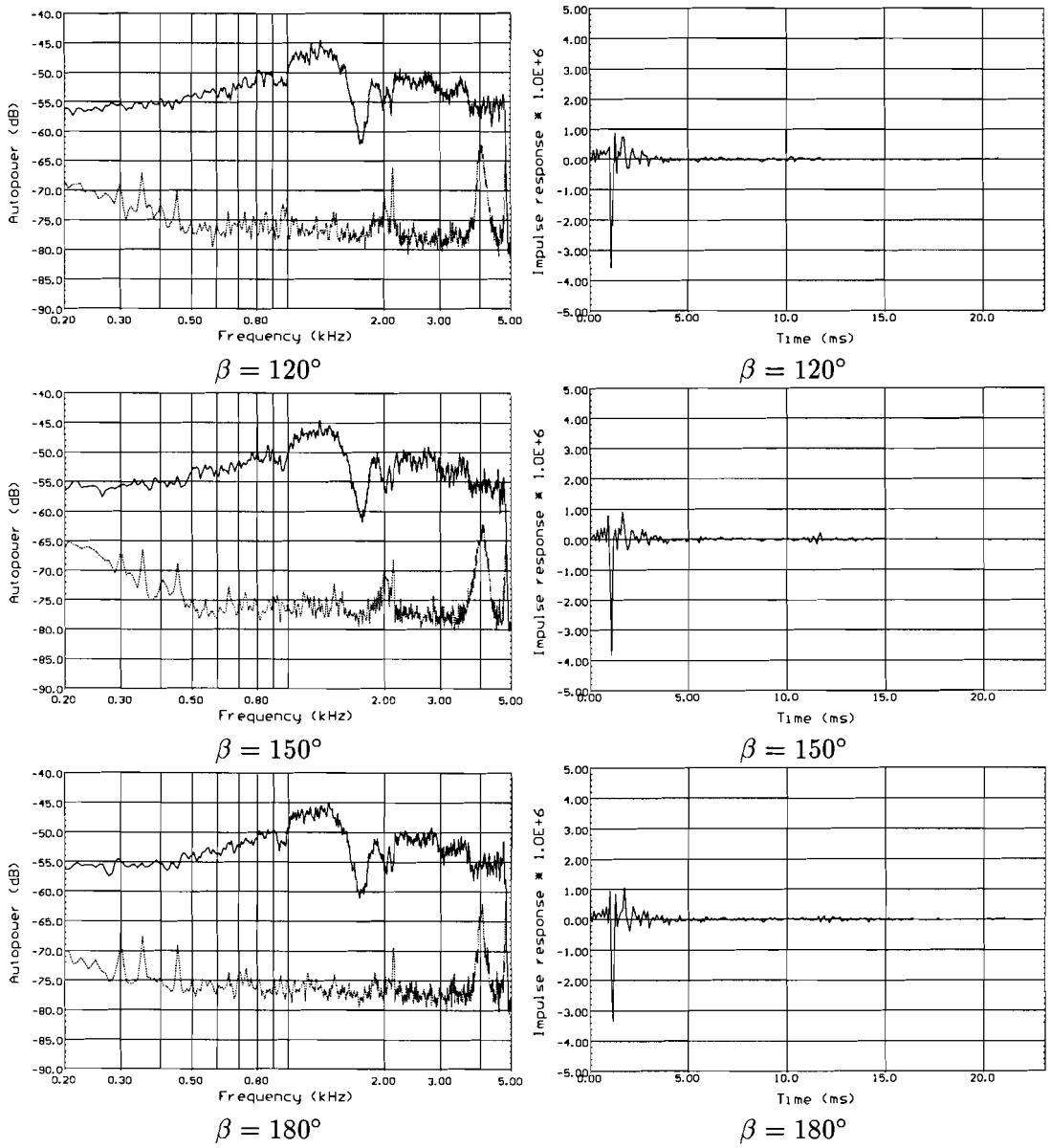

Figure 6.3: Results from measurements using an adaptive noise canceller. The pictures on the left side show the microphone power before (solid) and after cancellation (dashed). The pictures on the right side show the adaptive filter weights.

6.2 Conclusions

A real time implementation of the filtered-x algorithm has been tested is an active noise cancelling setup. Measurements show that the adaptive system used is able to reduce the sound pressure obtained by the error sensor over a wide frequency range. Before this is possible an estimation of the auxiliary transfer function of the adaptive system has to be made for stable operation. Several conclusions can be drown from the obtained results:

- The cancellation of the primary sound field by introducing a secondary sound field is not complete since a residual microphone signal exists. Part of this can be explained by looking at the dynamic range of the ADC's. The aim of introducing a cancelling signal is to reduce the signal produced by the microphone. This automaticly means that quantization error made by the ADC which measures this signal becomes relatively lager. Then of course there is the limitation of working with finite accuracy of calculation performed by the DSP, noisy amplifiers, using a FIR model instead of a model which also has poles etc. etc..

- In average, a reduction in microphone power of 20 dB is obtained for every angle of β.

- The resulting filter coefficients are stable meaning that the algorithm used is stable.

- It can be seen from the outcome of the resulting adaptive filter weights depicted in Figs. 6.2 and 6.3 that the formed filter mostly exists of a negative delay, compensating the difference in distance between the primary source to microphone and the secondary source to microphone. Since this difference in distance is maintained constant throughout the hole experiment the resulting solution for the adaptive filters all look the same.

Chapter 7

Multiple point cancellation

An observer can sense the direction from which the sound originates due to the time and level difference between ear signals (other aspects are involved but they are not relevant to be discussed in this report). To simulate a human observer, two detectors (representing the ears) should be used. In the last chapter it was shown that a relatively large reduction was achieved by using just one secondary source to control the primary sound field. It is however, not possible to create a phantom source with a single secondary source and a single microphone.
In this chapter an experiment will be described using two secondary sources to control the primary sound field in the vicinity of two microphones. In order to construct such a practical adaptive controller, some measurable error criterion has to be defined. In [4] a multiple LMS algorithm is presented which uses a gradient decent method to minimize the sum of the squared error signals. The first part of this chapter will describe the presented method in [4]. After this results from experiments using this multiple error algorithm will be presented.

7.1 Multiple error LMS algorithm

In the practical system illustrated in Fig. 7.1, two adaptive digital filters are used to operate on the input signal $x[k]$ and drive the secondary sources $(f_1[k], f_2[k])$ in such a way that sum of the squared outputs from the error microphones $(e_1[k], e_2[k])$ are minimized. In [4] this signal processing problem is assessed and an algorithm is presented which is an extended case of the filtered-x algorithm used in the last chapter.

Note
It was stated in [4] that there should at least be as many error sensors as there are secondary sources (and so adaptive controllers). The algorithm used will then result in a unique solution. When however, a situation would arise where the number of secondary sources is bigger then the number of error sensors, this will not be the case. The adaptive controllers will influence each other and will most likely never stabilize. The other way around

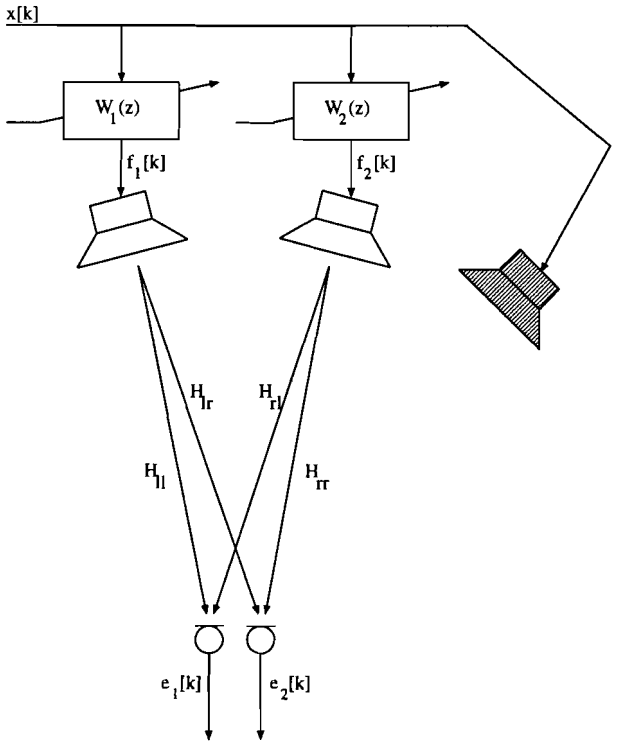

Figure 7.1: Two secondary sources are used to control the primary sound field at the position of the two microphones.

however, will not cause problems.

The cost function to be minimized is now defined as the sum of the mean squared errors and is given by

$$J = E\{e_1^2 + e_2^2\}. \tag{7.1}$$

The total error is a quadratic function of each of the filter coefficients of $W_1(z)$ and $W_2(z)$. The optimum set of weights required to minimize J may therefor be evaluated adaptively using a gradient descent method like LMS.

To find the optimal solution for the adaptive filters $W_1(z)$ and $W_2(z)$, each coefficient should be adjusted by an amount proportional to the negative of the gradient of the error function J. An adaptive algorithm that can be used for this purpose is

$$\begin{aligned} \mathbf{w}_1[k+1] &= \mathbf{w}_1[k] - \alpha\,(e_1\hat{\mathbf{y}}_{11}[k] + e_2\hat{\mathbf{y}}_{12}[k]) \\ \mathbf{w}_2[k+1] &= \mathbf{w}_2[k] - \alpha\,(e_1\hat{\mathbf{y}}_{21}[k] + e_2\hat{\mathbf{y}}_{22}[k])\,. \end{aligned} \tag{7.2}$$

Here $\mathbf{w}_1[k]$ and $\mathbf{w}_2[k]$ are $N \times 1$ coefficient vectors of resp. $W_1(z)$ and $W_2(z)$ at time instant k. The signal vectors $\hat{\mathbf{y}}_{11}[k], \hat{\mathbf{y}}_{12}[k], \hat{\mathbf{y}}_{21}[k]$ and $\hat{\mathbf{y}}_{22}[k]$ each hold N filtered-x reference samples. To produce these signals, the estimations of the transfer functions between the secondary loudspeakers and the

microphones have to have to be known. Fig. 7.2 shows a block diagram of adaptive controllers $W_1(z)$. A similar diagram can be given for $W_2(z)$ where instead of $\hat{H}_{ll}$ and $\hat{H}_{lr}$, $\hat{H}_{rl}$ and $\hat{H}_{rr}$ are used.

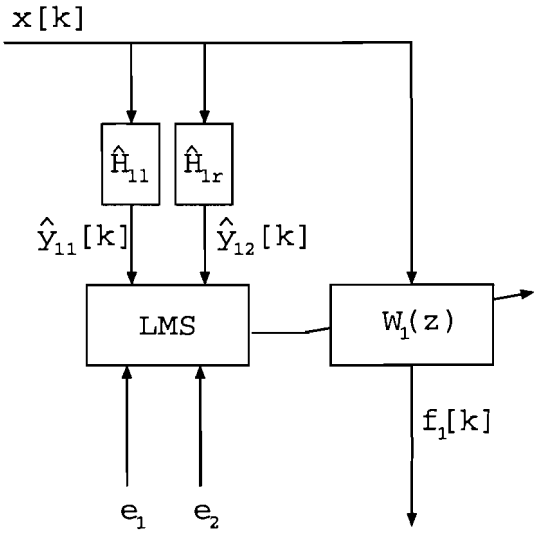

Figure 7.2: Adaptive controller using a multiple error algorithm. The transfer function $\hat{H}_{ll}$ and $\hat{H}_{lr}$ are estimations of resp. H_{ll} and H_{lr}.

In [4] a further analysis of this algorithm is given, showing that in average the coefficients of the adaptive filters converges to the optimal solution.

7.2 Practical experiment using the multiple error filtered-x algorithm.

Before the practical experiment can be conducted, the transfer functions between the secondary sources and the microphones have to be determined just like was done in the single error filtered-x algorithm. This means that for the setup depicted in Fig. 7.1, the transfer functions H_{ll}, H_{lr}, H_{rl} and H_{rr} have to be estimated prior to control. These estimations can than be copied in front of the LMS update unit as illustrated in Fig. 7.2.

The implementation for this experiment was done on two separate digital signal processors, one for each adaptive filter. The complete setup is shown in Fig. 7.3. The transfer function from each secondary source loudspeaker to each error microphone were modelled with 256 taps FIR filter during an initialization phase of the program. These filters were subsequently used to generate the reference signals $\hat{\mathbf{y}}_{11}[k], \hat{\mathbf{y}}_{12}[k], \hat{\mathbf{y}}_{21}[k]$ and $\hat{\mathbf{y}}_{22}[k]$. The implementation was done on two DSP56002 processors both operating at 70 MHz. The output signal from the adaptive filters where converted using 16 bit Digital to Analog converters. These signals where applied to an amplifier to drive the two secondary loudspeakers. The input signal $x[k]$ was

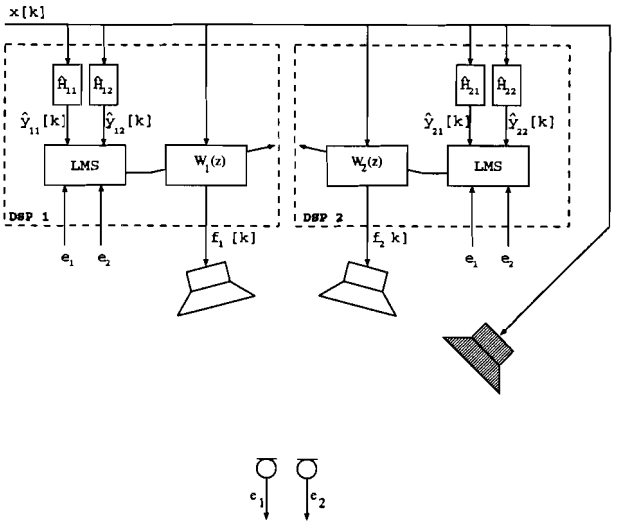

Figure 7.3: Used setup to test the multiple error LMS algorithm.

amplified to drive the primary loudspeaker. The error signals, $e_1[k]$ and $e_2[k]$ where sampled using $16bits$ analog to digital converters at a sample rate of 11025 Hz. The secondary loudspeakers are placed at 176 cm from the dummy head and are separated by a distance of 34 cm from each other. The primary loudspeaker is placed at 220 cm from the head at an angle β from the main axe.

The tasks DSP1 has to carry out every sample period are:

- Calculate the reference signals:

$$\hat{y}_{11}[k] = \sum_{n=0}^{255} x[k-n]\hat{h}_{n11},$$

$$\hat{y}_{12}[k] = \sum_{n=0}^{255} x[k-n]\hat{h}_{n12},$$

- Calculating the secondary source signal

$$f_1[k] = \sum_{n=0}^{255} x[k-n]w_{n1}[k],$$

- Updating the adaptive filter coefficients using

$$\mathbf{w}_1[k+1] = \mathbf{w}_1[k] - \alpha\left(e_1\hat{\mathbf{y}}_{11}[k] + e_2\hat{\mathbf{y}}_{12}[k]\right).$$

Here $\hat{h}_{n11}$ denotes the n^{th} coefficient of the estimated transfer function $\hat{H}_{11}(z)$ represented in the time-domain.
When the number of coefficients of the adaptive filter becomes bigger while maintaining the length of the estimations of the transfer functions between the secondary sources and the microphones, the number of calculations that have to be made by the DSP goes up very quickly. Since al these calculation have to be performed within one sample period (=90.7 μs) it is very difficult

to enlarge this amount. When the complete audio spectrum was to be used (20 Hz to 20 kHz) the sample frequency should at least be raised by a factor four meaning that the sample period goes down by this same factor.

7.3 Results

Fig. 7.4 and Fig. 7.5 show on the left hand side the power spectrum of the left microphone signal before (solid line) and after cancellation (dashed line) and on the right hand side the power spectrum of the right microphone signal before (solid line) and after cancellation (dashed line).
It follows from these results that an implementation of the multiple error algorithm performs well and that a large reduction in power is achieved for both microphones. The average amount cancellation obtained is more than 20 dB from every angle of β. The results also show that for low frequencies (200 Hz to 1kHz) the power reduction is lower than for frequencies above this region.

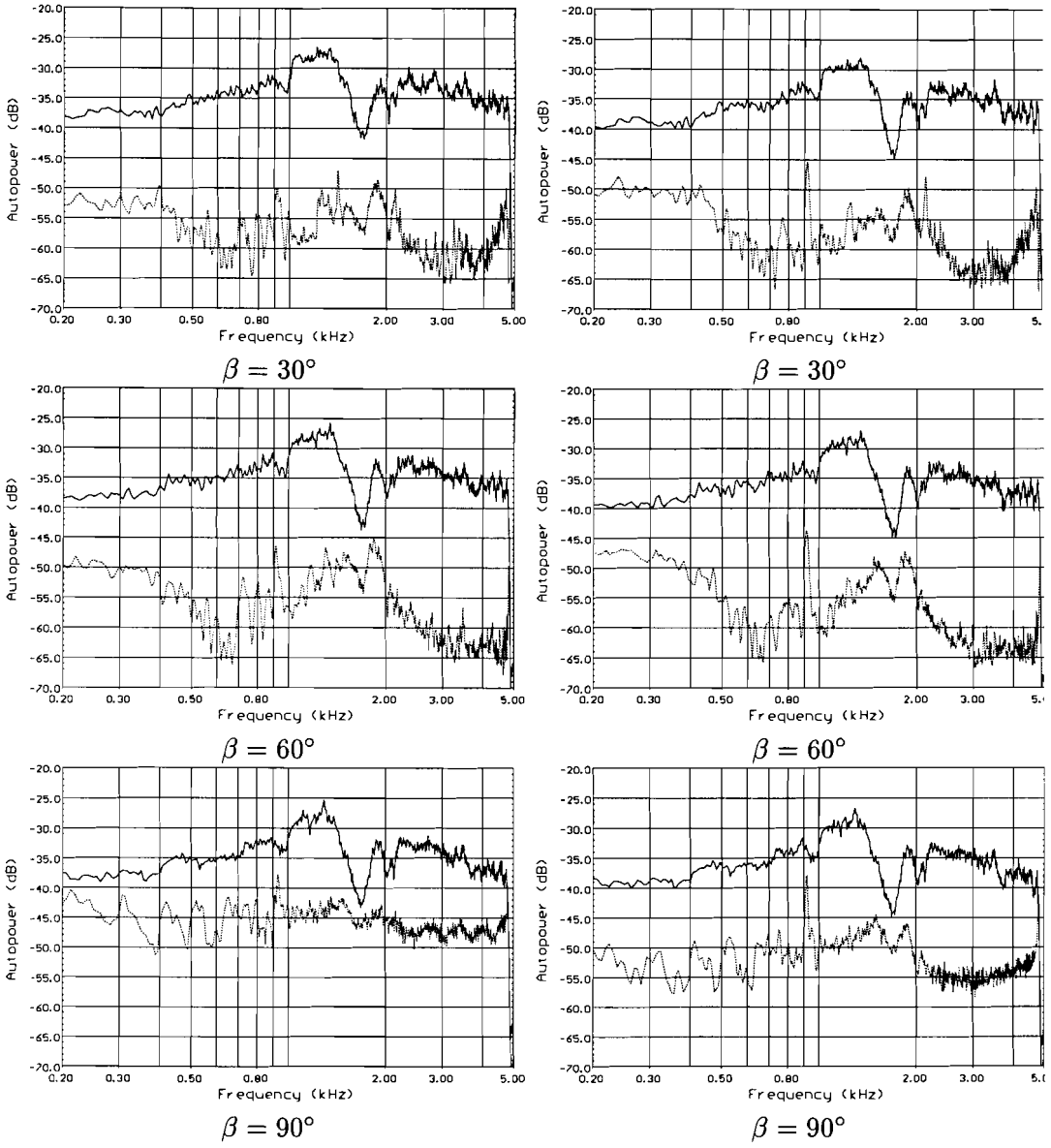

Figure 7.4: Results from measurements using an adaptive noise canceller. The pictures on the left side show the left microphone power before (solid) and after cancellation (dashed). The pictures on the right side show the right microphone power before (solid) and after cancellation (dashed).

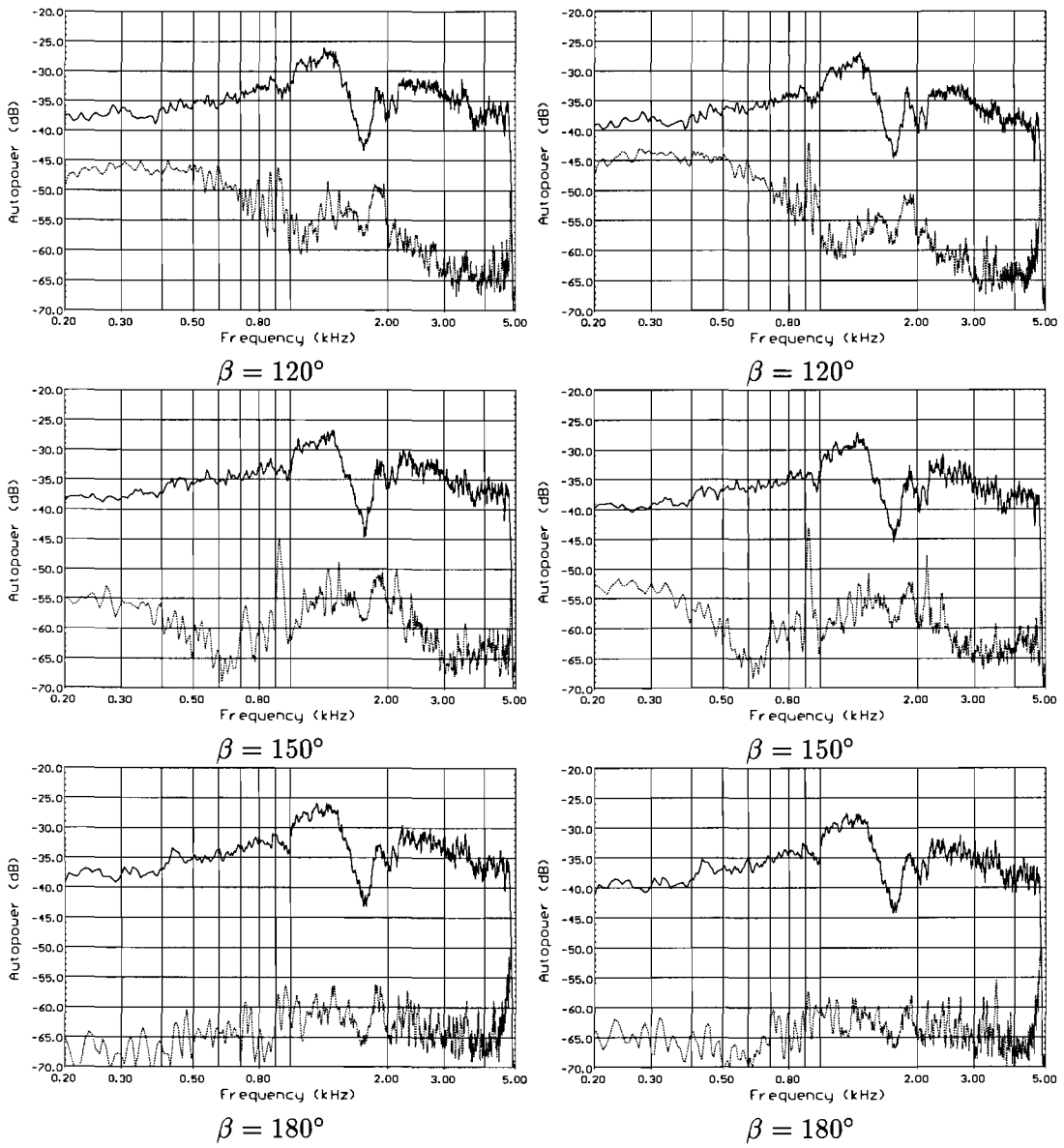

Figure 7.5: Results from measurements using an adaptive noise canceller. The pictures on the left side show the left microphone power before (solid) and after cancellation (dashed). The pictures on the right side show the right microphone power before (solid) and after cancellation (dashed).

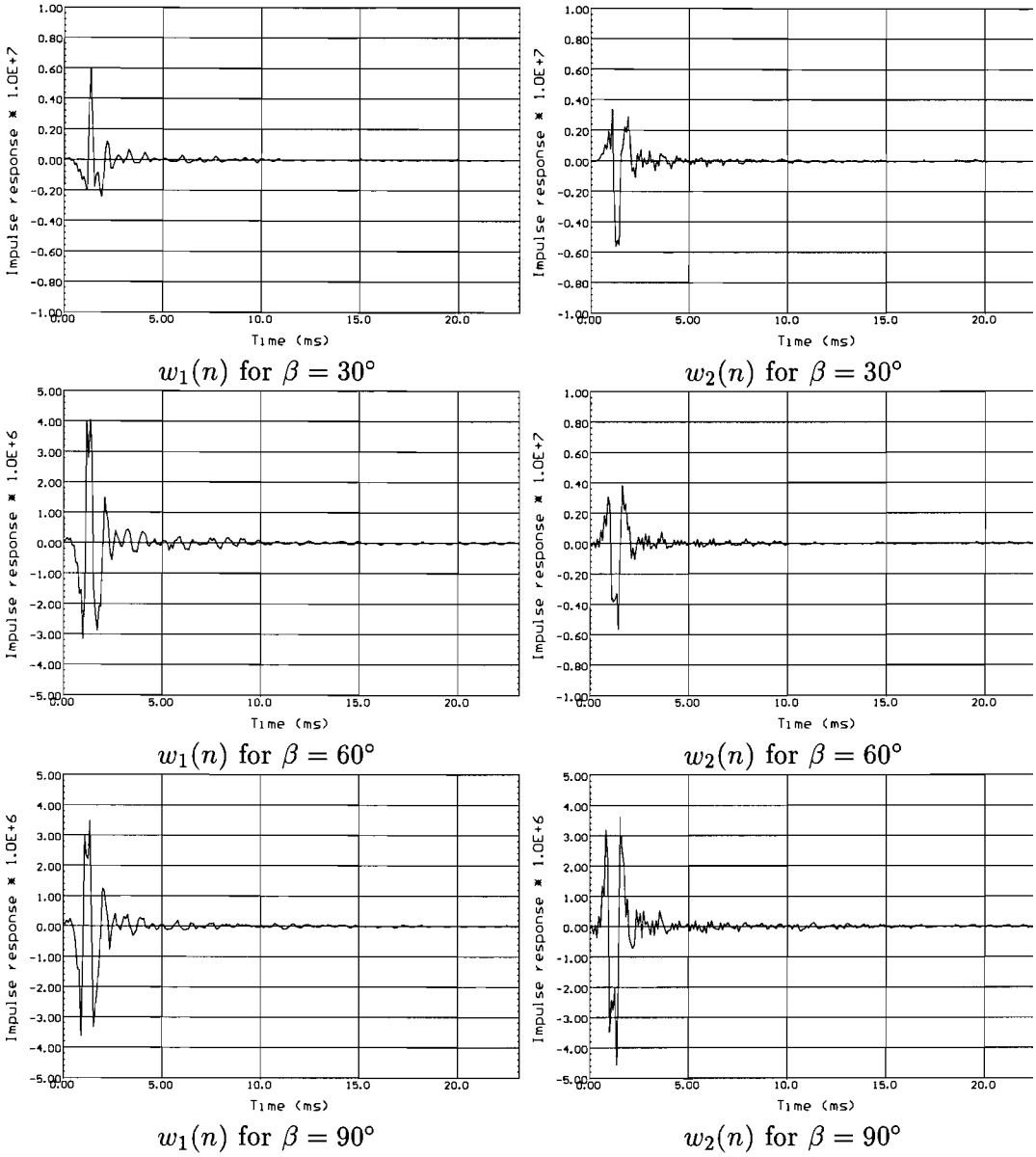

Figure 7.6: Left: impulse response of $w_1(n)$ after system stabilized. Right: impulse response of $w_2(n)$ after system stabilized.

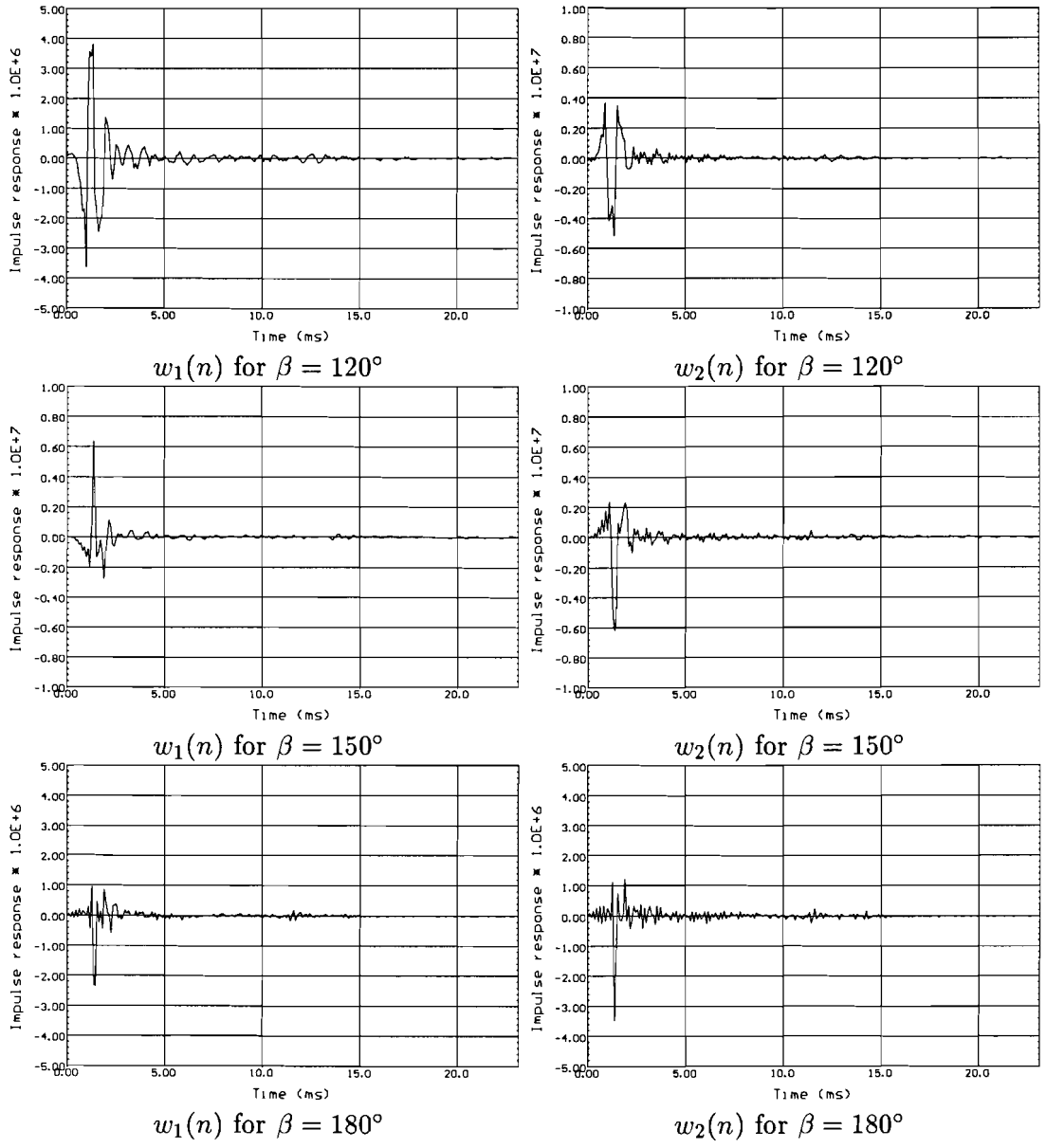

$w_1(n)$ for $\beta = 120°$ $w_2(n)$ for $\beta = 120°$

$w_1(n)$ for $\beta = 150°$ $w_2(n)$ for $\beta = 150°$

$w_1(n)$ for $\beta = 180°$ $w_2(n)$ for $\beta = 180°$

Figure 7.7: Left: impulse response of $w_1(n)$ after system stabilized. Right: impulse response of $w_2(n)$ after system stabilized.

7.4 Perception

In order to determine the acoustical effect produced by the secondary sources, the filters were frozen, the primary source removed and microphones replaced by a real observer. Although microphones instead of real human ears were used to produce the error signals, the effect obtained was remarkable. For small angles of β (up to 60°) the perception of the phantom source was very realistic. For angle β greater than 60° the subjective localization of the phantom source became more difficult. Still it can be sad that already when using two microphones instead of real ear canals a good effect is created. This experiment also shows that the idea of creating phantom sources using an active noise controller works and that an aperture enlargement is perceived.

7.5 Conclusion

An algorithm for the adjustment of the secondary sources using the method of steepest descent has been described and tested in a real time active noise control experiment. The algorithm minimizes the sum of the mean squared output of the error sensors. Prior to the actual active control, estimations of the transfer functions between secondary sources and error microphones have to be made to stabilize the algorithm.
The results from the experiments, conducted in an anechoic environment, show that a large reduction in microphone power can be obtained using this multiple error LMS algorithm.
It was found that the resulting impulse responses of the two adaptive filter are largely determined by the difference in distance between the primary source and the secondary sources.
Although intensive localization test still have to be performed it is shown that the idea of using an active noise controller to determine the filters needed to create phantom sources works.

Chapter 8

Creating phantom sources

The aim of this project was to create phantom sound sources using an adaptive system. To accomplish this, it was suggested to use the approach of creating an active noise controller which compensates a primary sound field by introducing secondary sound fields. The results from the experiments presented in the last chapter show that an array of two adaptive filters driving two secondary sources are able to obtain a large reduction is sound pressure in the vicinity of the two microphones serving as error sensors. For the creation of phantom sources however, a more realistic method should be used where the microphones are replaced by a real human head with small error sensors in the ears. Since experiments using real test persons are very costly and difficult to conduct (microphones have to be placed in the ear channel), an artificial head is used instead.

8.1 Practical experiments using a dummy-head

The setup for this experiment differs slightly from the one described in the last chapter (see Fig. 8.1). The microphone are replaced by a B & K dummy head and placed at 150 cm from the secondary speakers. The primary speaker is, once more, placed on a movable stand and rotated in a plain around the head while maintaining a constant distance of 220 cm from the middle of the head. Again, prior to control the transfer function from secondary sources to the ears are estimated and used to generate the reference signals.

8.2 Results

Fig. 8.2 and Fig. 8.3 show the relevant part of the power spectrum of the error signals e_1 and e_2 before (solid line) and after cancelation (dashed line) for several angle of β. The dashed-dotted lines in these plots show the noise in the system caused by noisy amplifiers, noisy microphones and other disturbances. It is found that the sound pressure level at the left ear before cancellation becomes smaller when the angle β is enlarged. Obviously, this is caused by the head which attenuates the sound before it is picked up

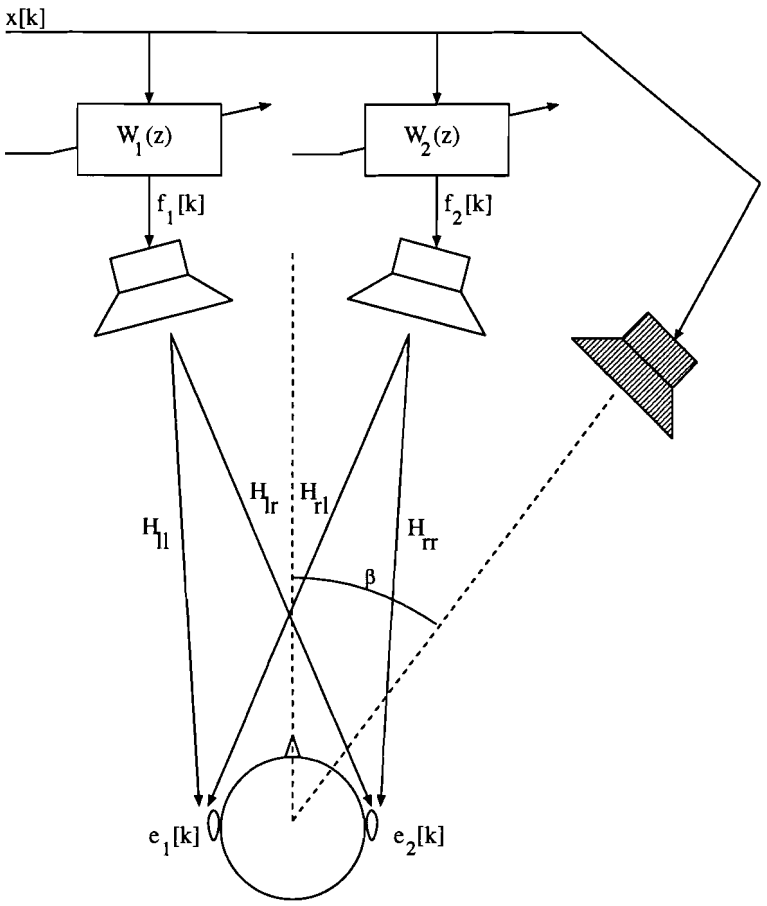

Figure 8.1: Experimental setup using a dummy head with microphones in the ears as an observer.

by the microphone. The relative pressure drop for this is ear decreased to almost 10dB instead of 20dB. This problem can be solved by increasing the amplification factor for this microphone. Before doing this however, test should be done checking if it is relevant for the perception.
Fig. 8.4 and Fig. 8.5 show the impulse responses of resp. $w_1(n)$ and $w_2(n)$ as a function of time.

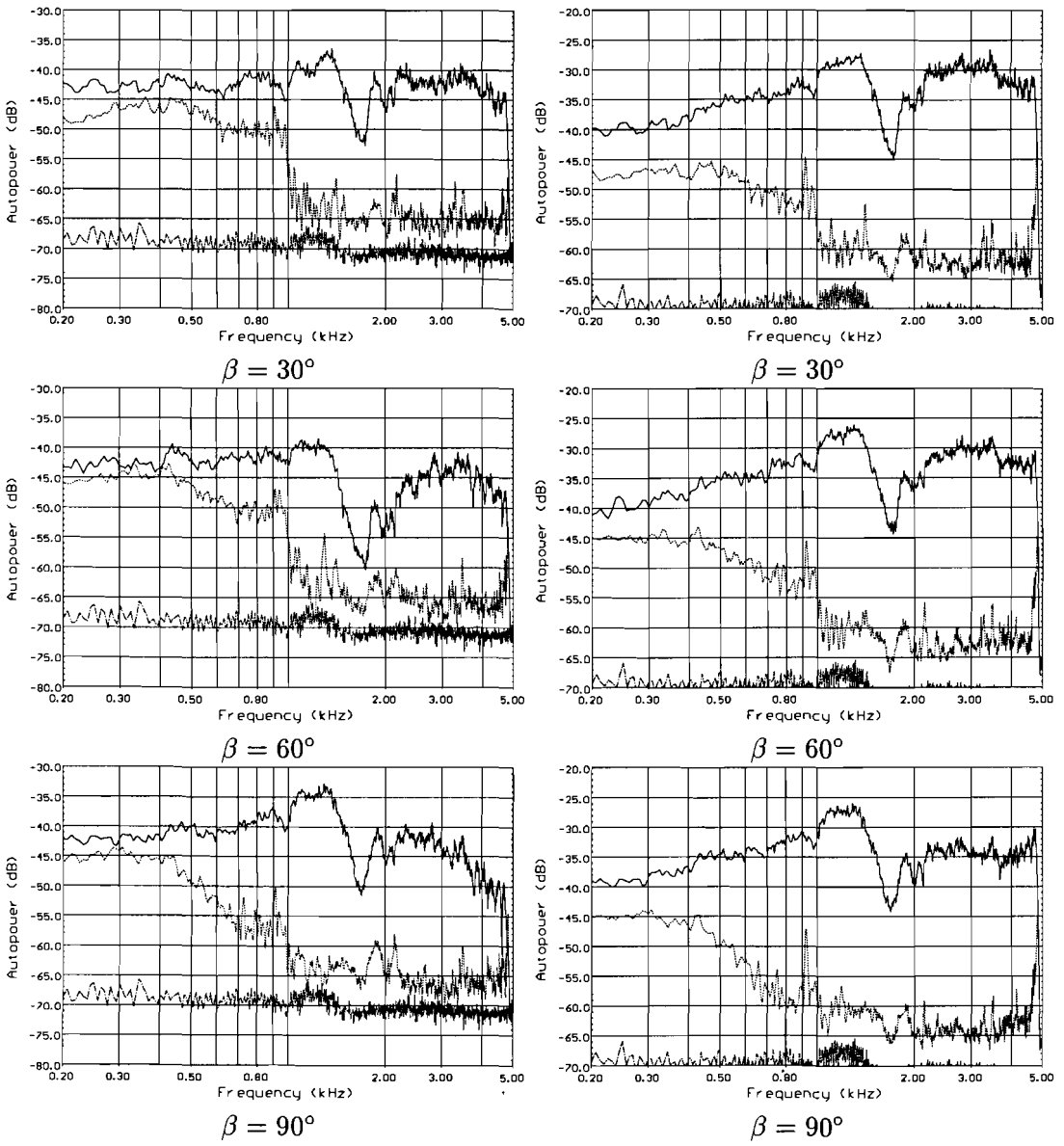

Figure 8.2: Results from measurements using an adaptive noise canceller. The pictures on the left side show the left microphone (left ear) power before (solid) and after cancellation (dashed). The pictures on the right side show the right microphone (right ear) power before (solid) and after cancellation (dashed). The dashed-dotted lnes denote the noise measured when no loudspeaker is radiating.

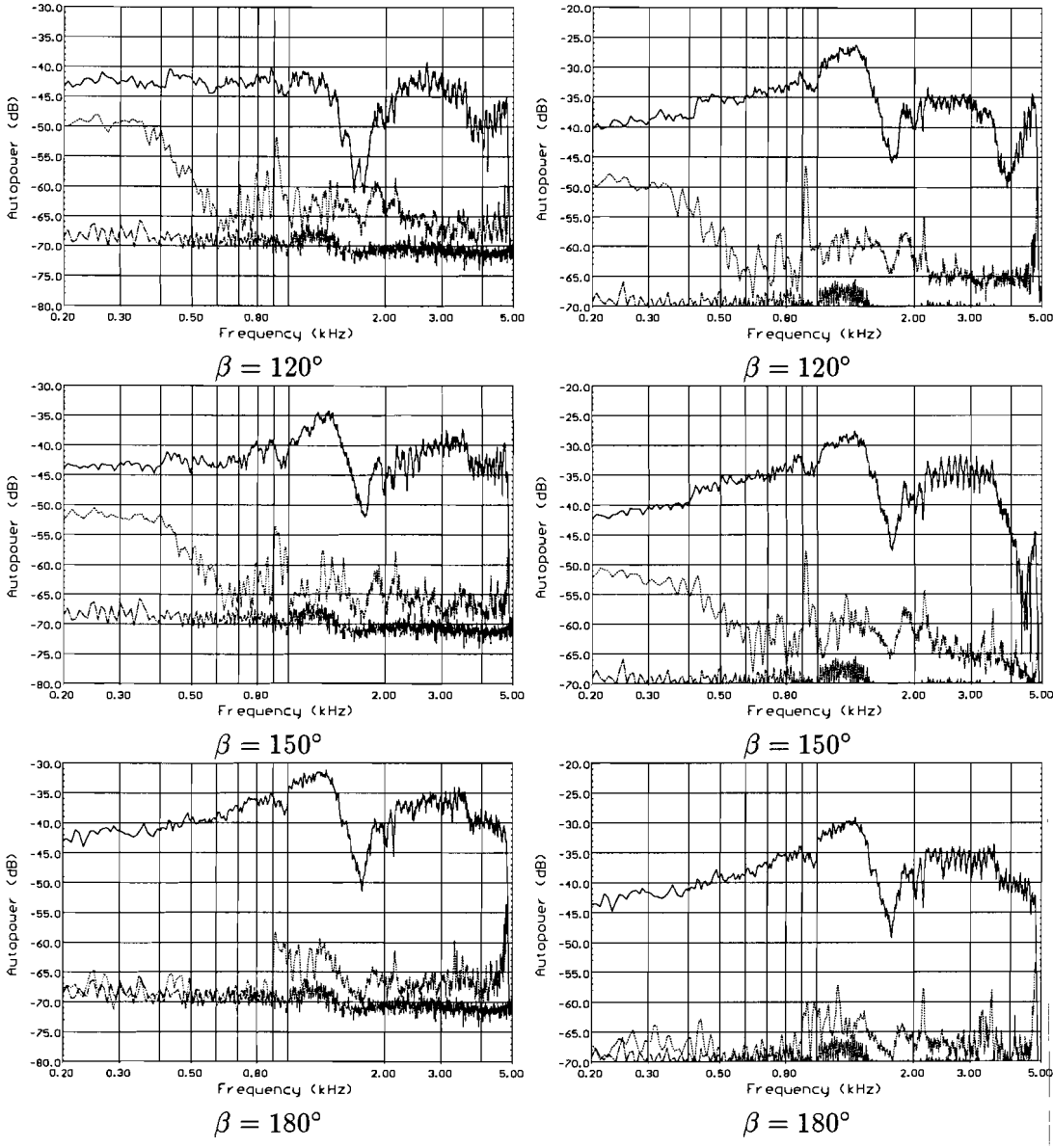

Figure 8.3: Results from measurements using an adaptive noise canceller. The pictures on the left side show the left microphone (left ear) power before (solid) and after cancellation (dashed). The pictures on the right side show the right microphone (right ear) power before (solid) and after cancellation (dashed).The dashed-dotted lnes denote the noise measured when no loudspeaker is radiating.

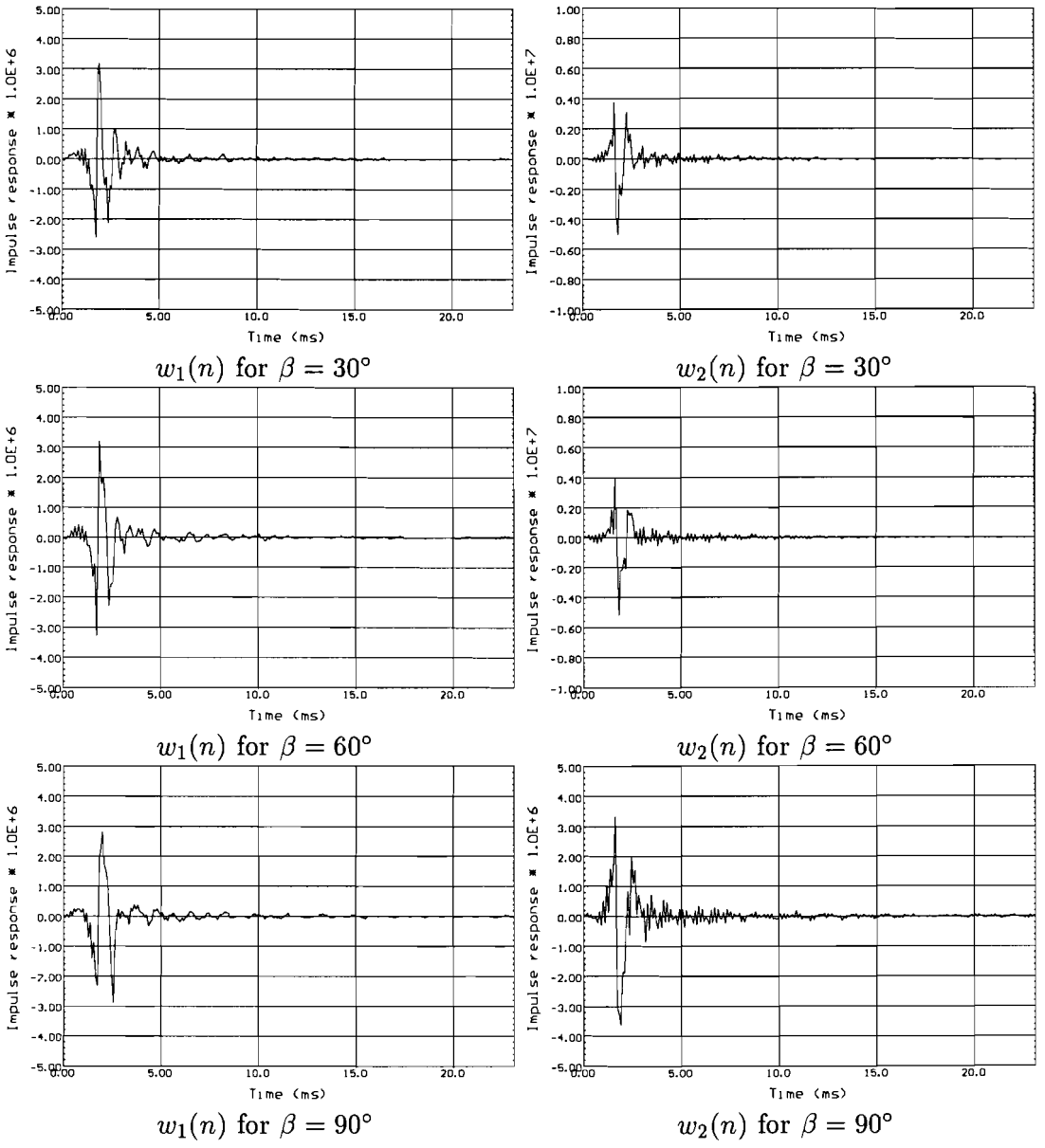

$w_1(n)$ for $\beta = 30°$ $w_2(n)$ for $\beta = 30°$

$w_1(n)$ for $\beta = 60°$ $w_2(n)$ for $\beta = 60°$

$w_1(n)$ for $\beta = 90°$ $w_2(n)$ for $\beta = 90°$

Figure 8.4: Left: impulse response of $w_1(n)$ after system stabilized. Right: impulse response of $w_2(n)$ after system stabilized.

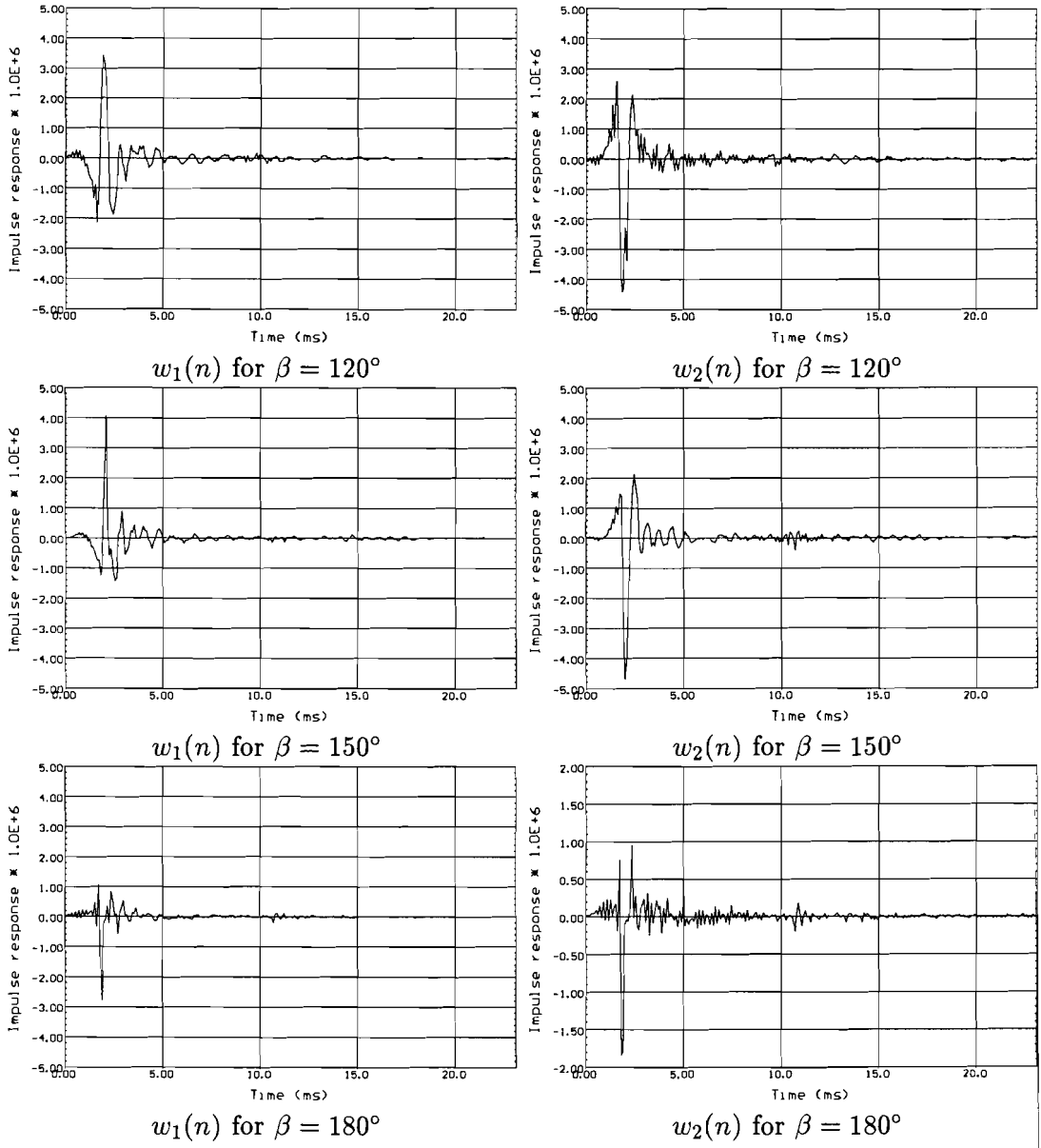

Figure 8.5: Left: impulse response of $w_1(n)$ after system stabilized. Right: impulse response of $w_2(n)$ after system stabilized.

8.3 Perception of direction

The idea of using an active noise controller to cancel the out the primary signal, freeze the filter coefficients and remove the primary source to create phantom sources can now be tested. The impulse responses presented in the last section where obtained using a dummy head instead of a real head. Globally it can be sad however that, when dummy "observer" is replaced by a real human observer a aperture enlargement is experienced. Additional experiments should be conducted, testing the perception of a number of human observers. Before this is done however, the frequency range should be extended and the environment where the filters are determined should be changed to a more realistic surrounding. To do this the sample frequency should be raised and the length of the filter (number of taps) should be extended. It should not be forgotten that when the sample frequency is doubled while maintaining the number of taps, the impulse response is reduced by a factor of four. This is not possible with the time domain system used for the experiment described in the last section. The calculation time left within one sample period is to small. A solution to this problem may be found in a Block Adaptive Frequency Domain Filter. Here only part of the coefficients are update every sample period resulting in less calculation time.

8.4 Conclusions

The multiple error LMS algorithm is tested in a setup using a B & K dummy head as observer. An average reduction of 20 dB to 25 dB in ear pressure (= microphone power) is obtained when two secondary sources are used to compensate a primary source. It is show in Figs. 8.2 and 8.2 that the production of cancellation effect become more difficult at low frequencies. The resulting impulse responses depicted in Figs. 8.4 and 8.5 show again that a large part it is just a time delay compensating the difference in distance as was found in the experiments done with the single point cancellation (chapter 6).

Chapter 9

Loudspeaker simulation using headphones

When headphones are used to reproduce sound intended for a standard loudspeaker set-up, the precieved sound will appear to be coming from within the head since the directional information from the original construction is lost. This phenomena is a well studied topic and is known as In-the-Head Locatedness (IHL). If however, the headphone signals are processed so the sound precieved by the listener is the same as would be when using loudspeakers, the IHL problem disappears and a more natural situation appears. Fig. 9.1 shows the situation where two headphone speakers together with the two filters W_1 and W_2 simulate a speaker placed at a certain distance from the listener.

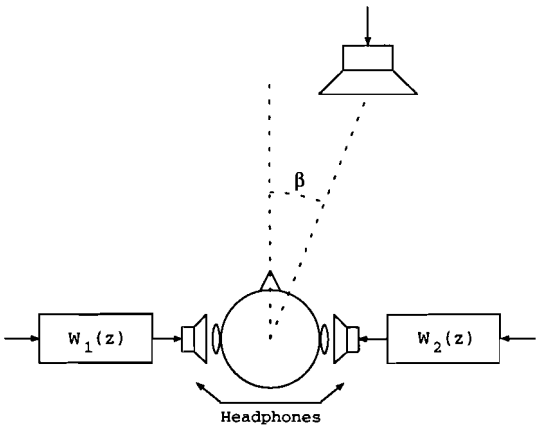

Figure 9.1: Loudspeaker simulation using headphones.

The problem discussed here is very similar to the problem outlined in the preceding chapters, where a phantom source was created using two secondary speakers. For this situation the secondary sources are the headphone speakers.
In this chapter a description will be given on how headphones can be used

to simulate a loudspeaker. After this an adaptive system, based on the experience of the preceding chapters, will be presented which determines the filters W_1 and W_2 in an adaptive manner.

9.1 Fixed filter correction for loudspeaker simulation

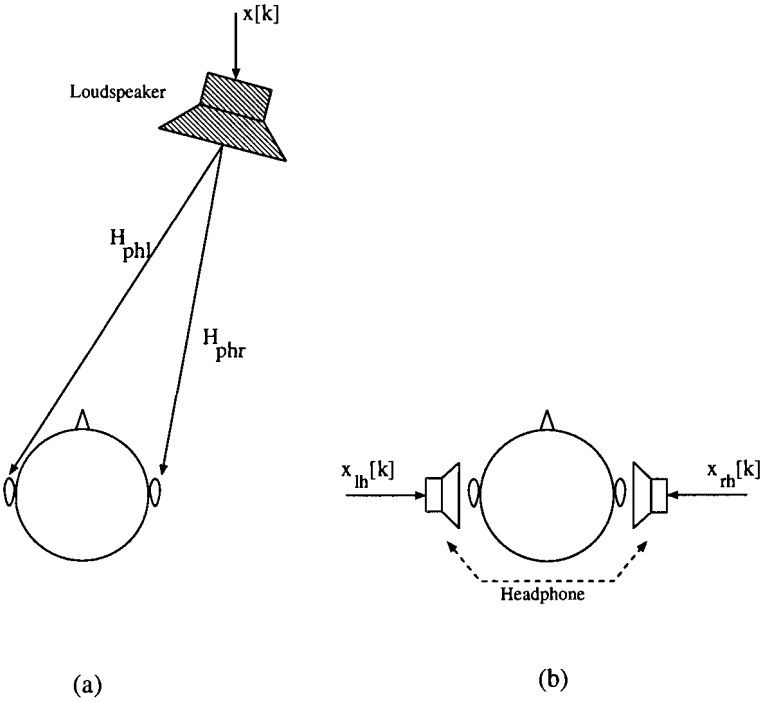

Figure 9.2: (a) observer listening to loudspeaker. (b) observer listening to simulated loudspeaker by means of a headphone.

Fig. 9.2(a) shows the situation where an observer is placed in front of a loudspeaker producing sound. In order to simulate this loudspeaker using a headphones, the pressure in the ears of the observer created by this speaker should be equal to the pressure created by the headphones. To solve this problem mathematically, the ear pressure for both situation should be calculated and made equal. This situation however, is similar to the situation discussed in Chapter 1.1 from this report. The only changes that have to be made are re-measuring the transfer functions from secondary sources to the ears since these sources are now placed close to the head. A simplification for this case can be made by assuming that there is hardly any cross-talk between signals from the left secondary source to the right ear and the right secondary source to the left ear. So, by making $H_{rl} = H_{lr} = 0$ and adopting Eq. (1.5) the filters W_1 and W_2 become:

$$W_1 = \frac{H_{phl}}{H_{ll}},$$

$$W_2 = \frac{H_{phr}}{H_{rr}}. \tag{9.1}$$

Theoretically this all seems very easy. Practically however, the same problems as with the creation of phantom sources using fixed filters have to be solved.

9.2 Adaptive filter correction for loudspeaker simulation

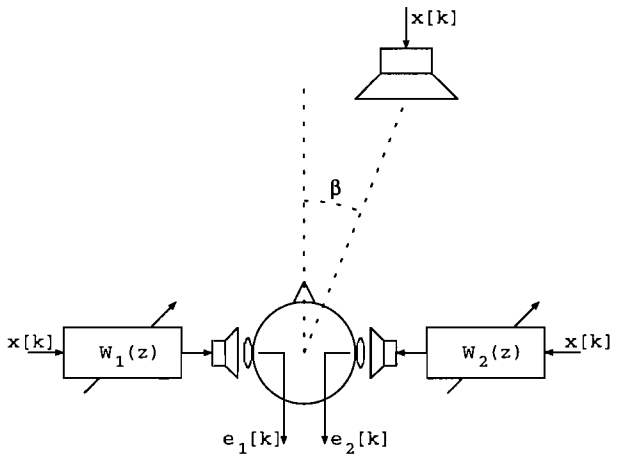

Figure 9.3: Loudspeaker simulation using headphones and two adaptive filters W_1 and W_2.

The idea of simulating a loudspeaker with the aid of headphones and adaptive filters is again based on active noise cancellation. This time the headphone speakers produce the secondary sound field which compensates the primary sound field in a reference point of the ear. When this is accomplished the adaptive process can be frozen and the primary speaker can be removed. The resulting filters W_1 and W_2 in combination with the headphone, now simulate the removed speaker. Theoretically this idea is very simple. For a practical situation however, the next problems have to be solved:

- The pressures at the ear drums have to be measured. This means placing small microphones in the ear canals of the subject to obtain the signals $e_1[k]$ and $e_2[k]$, which are needed for the update algorithm.
- Very "open" headphones has to be used to ensure that the listener can perceive the sound coming from the primary source. In the ideal situation, the observer would not sense any difference in sound pressure with or without the headphones. This however is not realistic for a practical situation and headphones should be used which changes the response between the primary source and the ears as less as possible.

When these problems are solved, the system created has several advantages compared with the system where two loudspeakers are used. Firstly, there is hardly any cross talk between left headphone speaker and right ear and between right headphone speaker and left ear. This means that the simple single point LMS algorithm discussed in Chapter 6 can be used. Secondly, the transfer function between for example left speaker and left ear does not change when the head is moved. So the instability problem discussed in Chapter 4 does not apply here anymore, if of course the phase error of the estimation is kept within limits.

9.3 Open headphones

If the idea of active noise cancelling is to be used to determine the transfer functions needed to simulate a loudspeaker, a headphone should be used which has a good frequency response, and which is "open" enough so the observer can perceive sound coming from the outside of the headphone. Measurements have been done using a dummy head as an observer "listening" to a speaker, producing white noise. To see what effect the selected headphones had on the transfer function between the speaker and the ears, the dummy head microphone signals where measured before and after the headphones where placed on the head. The results from these measurements are shown in Fig. 9.4. As can be seen from the pictures, the SONY headphones is the most "open" and change the transfer function the least. The SBC 3398 Philips however, is also very "open" and will be used for further experiments.

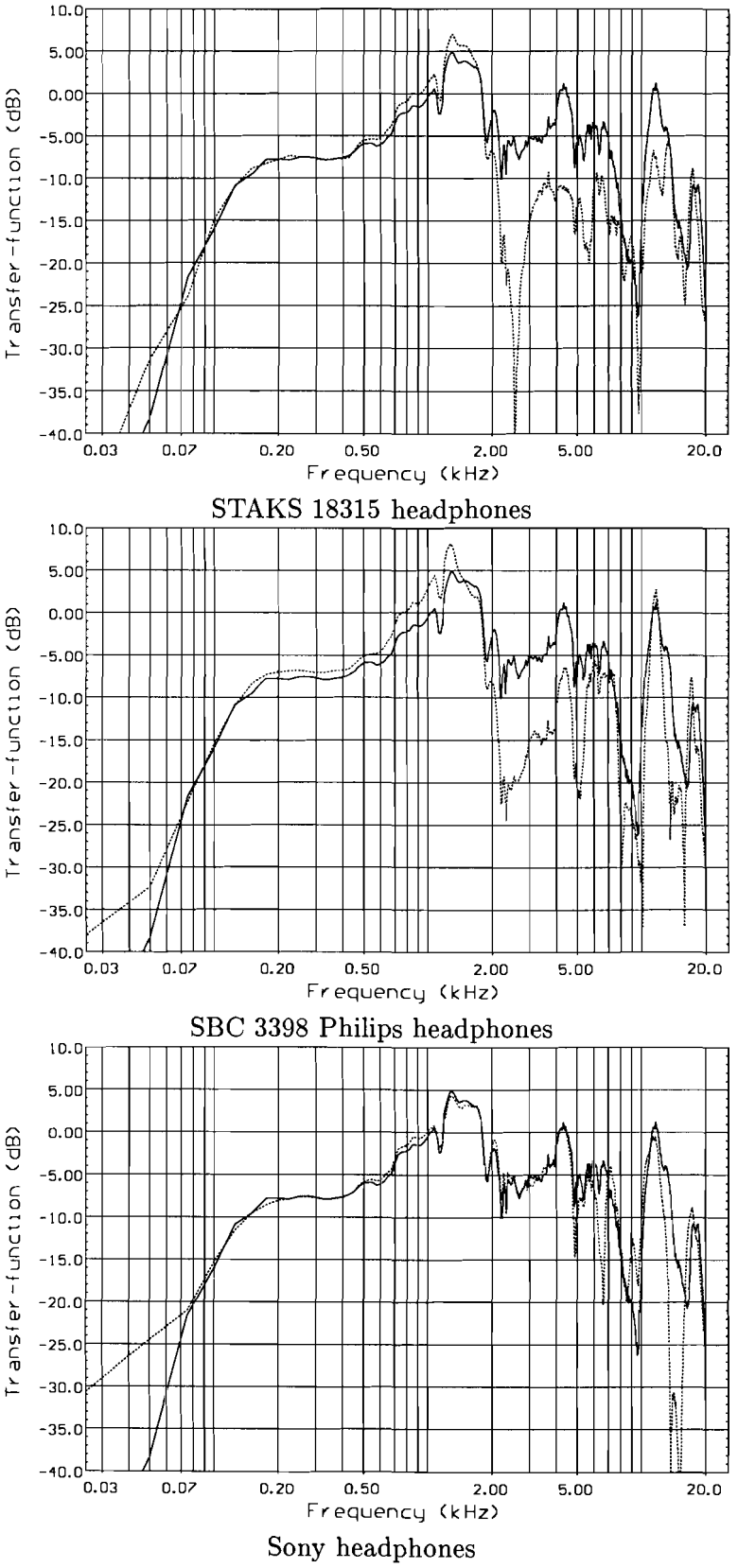

Figure 9.4: Transfer function between the speaker and the right ear microphone before (solid line) and after the various headphones are placed on the head (dashed line).

9.4 Microphones in ears

By placing microphone in an observers ear, the ear canal is changed and so the perceived sound. It is however necessary to place these error sensors in the ear of the observer to make sure that the cancellation takes place in a desired point in the canal. From the experiment described in this chapter small KNOWLES microphone with a small silicon tube attached to it. These microphones where glued to the inside of the headphone speakers so they would be on the desired position when the headphone is placed on the head.

9.5 Measurement setup

Referring to Fig. 9.3 an observer is placed in front of a speaker producing the primary sound field. The error signals e_1 and e_2 are measured with two small microphones which are glued to the inside of each headphone-speaker-shell. Using this construction makes sure that the microphones are always on the right position.
Before starting the adaption of the weights of $W_1(z)$ and $W_2(z)$ the transfer functions between the left ear and left speaker and right ear and the right speaker are estimated using a 128 taps adaptive filter. These filters are used to generate the reference signals as was described in Chapter 6. The implementation was done on two separate, individual DSP56002 signal processors both operating at 70 MHz. The signals coming from the microphones where amplified [1] and sampled with two 16 bits Analog to digital converters at a sample rate of 11025 Hz. The listener is placed at a distance of (about) 300 cm from the primary sound source on a rotatable chair. The adaptive controllers $W_1(z)$ and $W_2(z)$ both have 256 taps. Due to a poor microphone-headphone speakers below 1 kHz a band limited input signal from 1 kHz to 5kHz was used.

Comment
In the description of the setup with the single point cancellation in Chapter 6 was stated that for an ideal situation the transfer function of the cancelling adaptive filter ($W_1(z)$ for the left ear and $W_2(z)$ for the right ear) only compensates the difference between the distance from primary source to microphone and secondary source to microphone. The length of the adaptive FIR filter therefore determines the maximum area in which the observer can move.

9.6 Results

Using the system arrangement of Fig. 9.3 the transfer function between the microphone signals e_1 and e_2 and the (band limited) input signal $x[k]$ are measured before (solid line) and after cancellation (dashed line) and placed

[1] Schematics can be found in Appendix A

in Figs. 9.5 and 9.6. Again an average cancellation of 25 dB is achieved of every angle of β. Figs. 9.7 and 9.8 show the resulting adaptive coefficients from w_1 and w_2 after stabilization.
All these results where measured when the test person was sitting still without any head movement. It is however also possible to move the test persons head while the adaption mechanism is still updating the filters $W_1(z)$ and $W_2(z)$. When doing this the sound pressure in the ears first becomes larger since the sound generated by the secondary speakers are not in anti-phase anymore with the sound coming from the primary source. Then (depending on the speed of convergence) the sound pressure reduces again until a certain minimum is achieved.
During experiments it was also possible to view the filters coefficients while adapting. It is interesting to see how the impulse responses change when rotating the head or moving away from the primary speaker. Just by comparing the impulse response from $W_1(z)$ with that of $W_2(z)$ the angle between the primary source and the headphone could be determined. By looking at the peaks in the impulse responses, the distance from primary source to the headphones (actually secondary source) could be estimated. When looking at the results presented in Figs. 9.7 and 9.8 this same effect can be seen. When $\beta = 0°$ the peaks of $W_1(z)$ and $W_2(z)$ fall together. When the angle is enlarged the peak from $W_1(z)$ goes to the right and that of $W_2(z)$ goes to the left. At $\beta = 90°$ the effect changes and the peaks move back again. When $\beta = 180°$ is reached both the impulse responses have the same delay again.

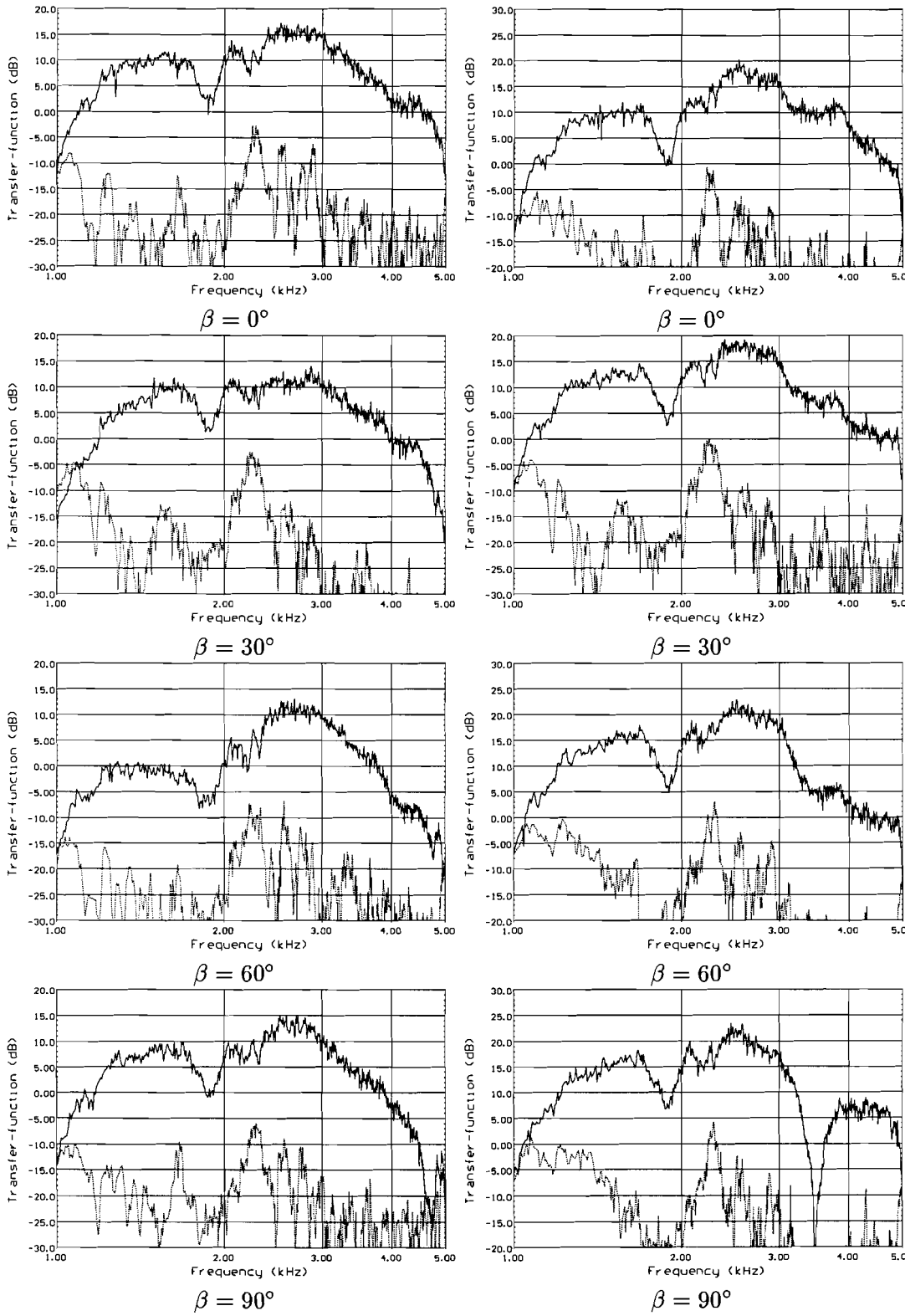

Figure 9.5: Mircophone signal before (solid) and after cancellation (dashed line).

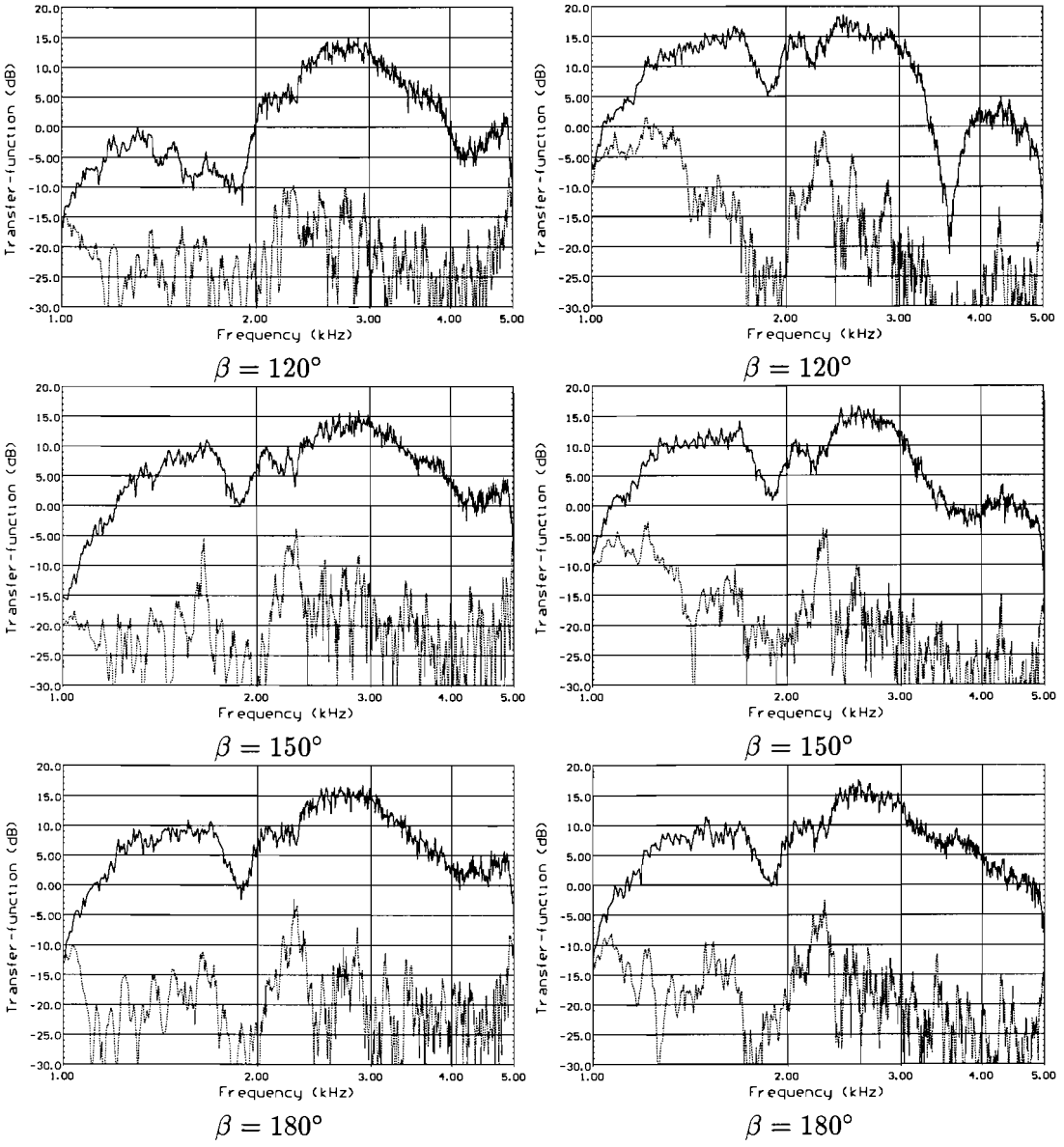

Figure 9.6: Mircophone signal before (solid) and after cancellation (dashed line).

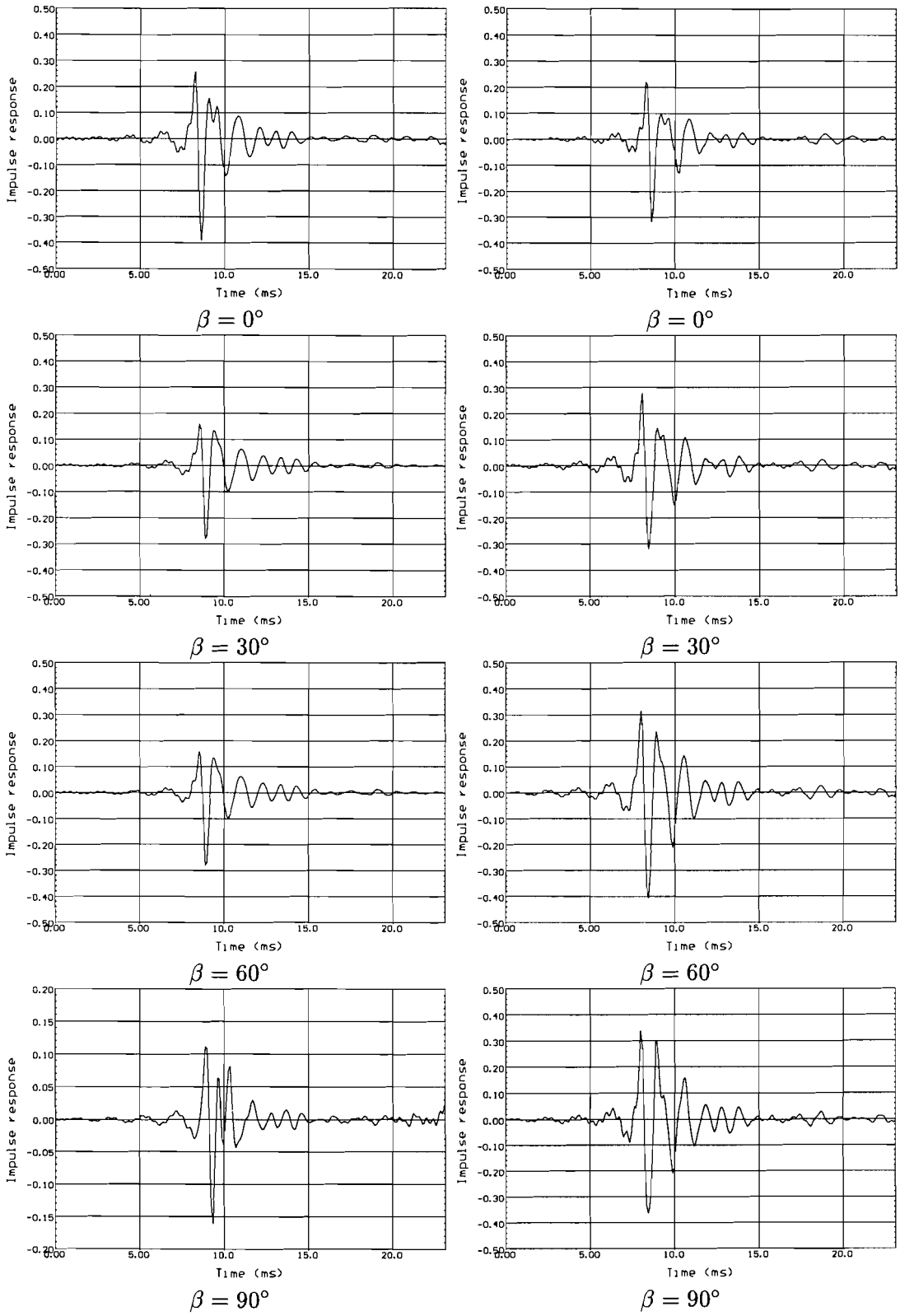

Figure 9.7: Impulse responses of $W_1(z)$ and $W_2(z)$.

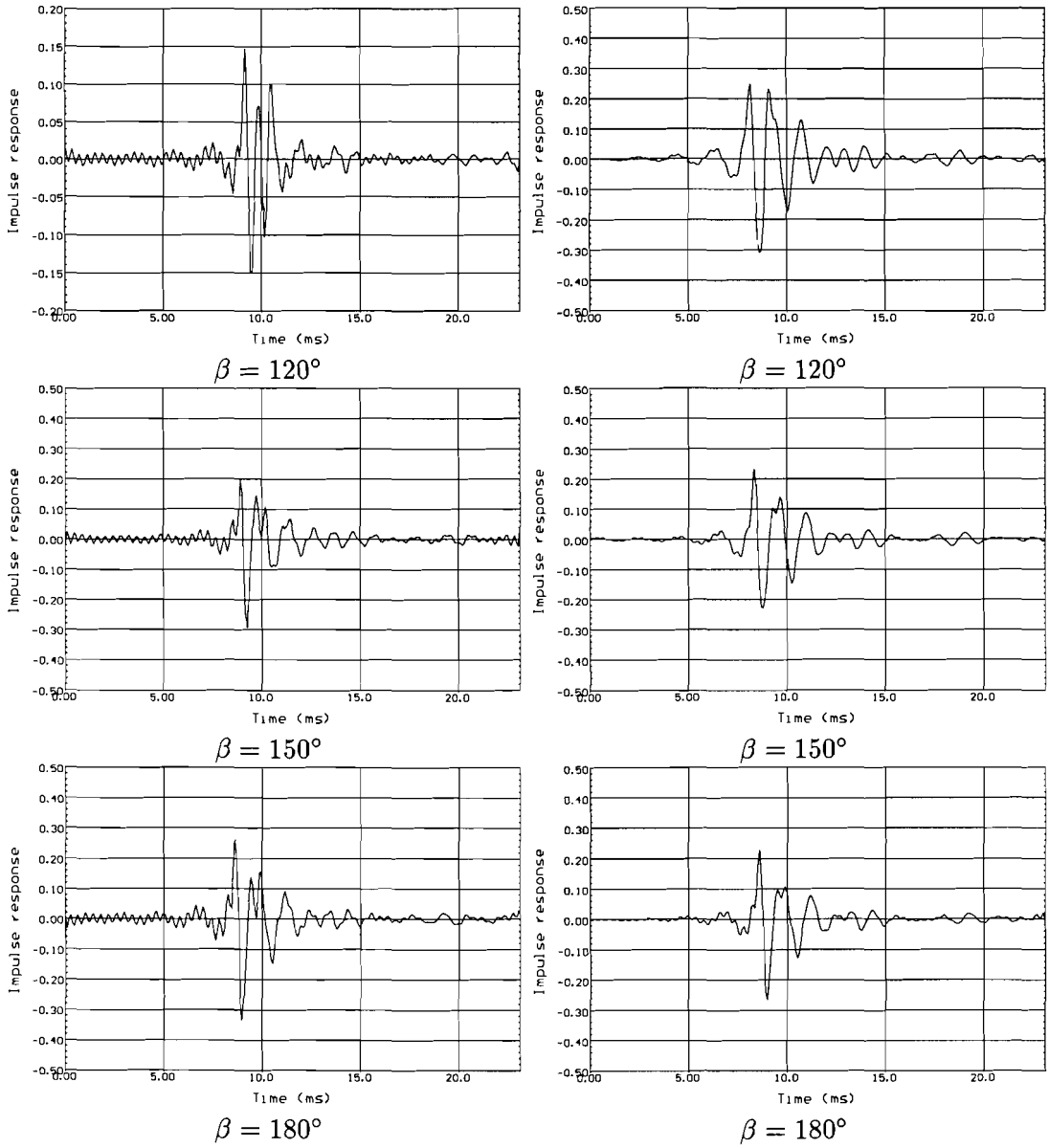

Figure 9.8: Impulse responses of $W_1(z)$ and $W_2(z)$.

9.7 Perception

The software that was used for the experiment described in the last section had an additional option where, after the adaptive system was stabilized and the adaption was switched off, the observer could listen to either the primary source or the secondary sources. By changing the input signal from white noise to e.g. music a nicer listening effect is obtained. A test was conducted in which several persons were asked to determine if the primary source or the secondary sources where creating the sound field. This is of course a very superficial test but it gives an indication if the idea of using headphones

to simulate a loudspeaker (or loudspeakers) works. the results from these test are that most of the tested persons could not tell the difference or, if asked, could not tell which source was playing. Its obvious that the effect obtained only works for the frequencies in the range from 1 kHz to 5kHz and that it has to be extended to the full audio bandwidth but still the setup used shows promising results and further research is recommended.

9.8 Conclusion

The idea of active noise cancelling and creating phantom sources with adaptive filters is used to simulate a loudspeaker via headphones. Since hardly any cross-talk between right ear and left headphone speaker and vise versa exists the single error filtered-x algorithm can be used. The results presented in this chapter show that a reduction of (in average) 25 dB is obtained and that the resulting transfer functions for $W_1(z)$ and $W_2(z)$ mainly consist of a delay. The idea of overcoming the IHL effect is tested by several persons in a listening test and in general it can be sad that the setup used gives good results.

Chapter 10

Future research

All the experiment described in the last chapters where conducted in a steady situation were the error sensor where not moving after initialization. In a more practical situation however, movement most be tolerated and problems resolving from the maximum allowed phase error of the estimation of the plant have to be solved. A real time estimator which automatically estimates the plant when the situation changes has to be developed.

The spatial extent of the effect of the system was not yet investigated. Until now a symmetric setup was used for experiments. It should however, also be tested how the system responds to a non-symmetric setup where the secondary sources are not equally spaced relative to the "observer".

Altough basic experiments have shown that the idea of creating phantom sources using the active noise cancelling approach works, more intensive test should be undertaken to see what the actual aperture enlargement is for several test-subjects.

The results from the simulation of loudspeakers using headphones are most promissing and futher reseach should be done on this topic. It would be interesting to see if the obtained transfer functions can be created using low-cost analog circuits.

Appendix A

Microphone amplifier

Microphone amplifier used for the loudspeaker simulation experiments.

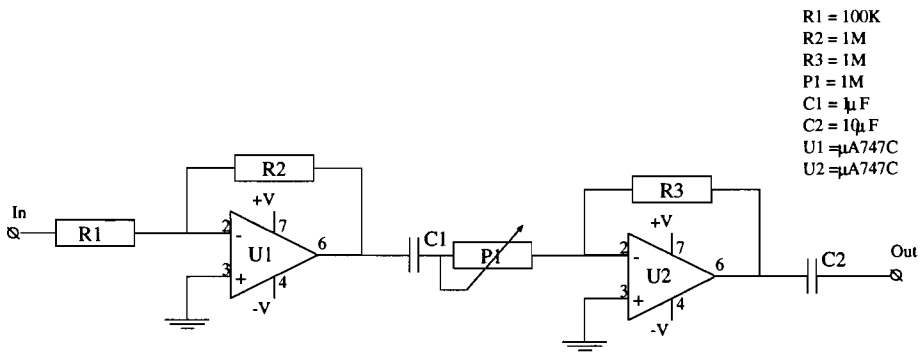

Figure A.1: Single microphone amplifier.

List of Figures

List of Tables

Bibliography

[1] R.M. Aarts. The generation of phantom sources. Technical report. 6794, Philips Research Labs., Eindhoven (Netherlands), 1994.

[2] C.C. Boucher, S.J. Elliott, and P.A. Nelson. Effect of errors in the plant model on the preformance of algorithms for adaptive feedforward control. *IEE Proceedings F*, 138(4):313–19, August 1991.

[3] S.J. Elliot. Active control of structure-borne noise. *J. of Sound and Vibration*, 177(5):651–673, Nov. 1994.

[4] S.J. Elliot, I.M. Stothers, and P.A. Nelson. A multiple error LMS algorithm and its application to the active control of sound and vibration. *IEEE Trans. on acoustics speech and signal processing*, 35(10):1423–34, 1987.

[5] S.J. Elliott, C.C. Boucher, and P.A. Nelson. The behavior of a multiple channel active control system. *IEEE Trans. on Ac. Speech and Sign. Proc.*, 40(5):1041–52, May 1992.

[6] R.E.A. Simons. *Onwards to phantom source generation by means of adaptive filtering.* Philips Research Laboratories Eindhoven (The Netherlands, YEAR = 1994.

[7] S.D. Snyder and C.H. Hansen. The influence of transducer transfer functions and acoustic time delays on the implementation of the LMS algorithm in active noise control systems. *J. of Sound and Vibration*, 141(3):409–24, September 1990.

[8] S.D. Snyder and C.H. Hansen. Design considerations for active noise control systems implementing the multiple input, multiple output LMS algorithm. *J. of Sound and Vibration*, 159(1):157–74, November 1992.

[9] S.D. Snyder and C.H. Hansen. The effect of transfer function estimation errors on the filtered-x LMS algorithm. *IEEE Trans. on Sig. Proc.*, 42(4):950–3, April 1994.

[10] P. Sommen. *Tijdsdiscrete signaalbewerking.* Number 5772. Faculty of Electrical engineering, 1993. Electronic Circuit Design (EEB).

[11] B. Widrow and S.D. Stearns. *Adaptive Signal Processing.* Prentice-Hall, Inc., Englewood Cliffs,, 1985.